UNIVERSIDADE FEDERAL DE ITAJUBÁ
PROGRAMA DE PÓS-GRADUACÃO EM ENGENHARIA DE ENERGIA

ENERGY STORAGE SIZING IN PV GENERATION SYSTEMS USING THE CONTI-VARLET METHOD AND DISUTILITY OPTIMIZATION

Paulo Alberto Viana Vieira

Itajubá, June of 2019

UNIVERSIDADE FEDERAL DE ITAJUBÁ
PROGRAMA DE PÓS-GRADUAÇÃO EM ENGENHARIA DE ENERGIA

Paulo Alberto Viana Vieira

ENERGY STORAGE SIZING IN PV GENERATION SYSTEMS USING THE CONTI-VARLET METHOD AND DISUTILITY OPTIMIZATION

A Thesis Presented to the Graduate School of the Federal University of Itajubá in Fulfillment of Requirements for the Degree of Master of Science in Energy Engineering.

Concentration area: Planning and Management of Energy Systems.

Supervisor: Edson da Costa Bortoni
Co-Supervisor: Arturo Sumam Bretas

June of 2019
Itajubá

DEDICATION

This work is dedicated to my parents, Moacir and Ivanide who have always given me their unconditional support.

To my beloved fiancé, Luana, who has accompanied me throughout this journey, standing by my side, encouraging me to be a better human being.

Finally, I would like to dedicate this thesis, especially to my son, Miguel, who gave me a particular motivation to continue working tirelessly.

Thanks for all their support, which without I could not have done.

ACKNOWLEDGMENTS

I want to acknowledge all the support that I have received throughout my graduate studies from my family and my friends. Without their constant support, especially from my parents and my fiancée, it would be impossible to do all the hard work which has led to this thesis.

I want to share my sincere gratitude to my supervisor, Professor Dr. Edson da Costa Bortoni, for his continuous support of my thesis, his patience, positive attitude, incredible wisdom, and guidance. Without his motivation and enthusiasm, the completion of this thesis would not have been possible. I could not have asked for a better advisor and mentor for my thesis, and I am forever thankful and in his debt. I also want to give thanks to my Co-Supervisor, Dr. Arturo Suman Bretas, for his encouragement, guidance, and support from the initial to the final level.

I am thankful to my committee members, Professor Dr. Akira Yamachita, Professor Dr. Marcos Vinicius Xavier Dias, for their valuable comments and suggestions during the preparation of this dissertation.

I acknowledge the support of all my colleagues and collaborators at the Federal University of Itajubá. I enjoyed the company of all members of the Excellence Center in Energetic Efficiency (EXCEN), who was part of a unique environment for sharing knowledge, curiosity, and a delicious coffee.

I want to acknowledge the CNPq, CAPES, INERGE, and FAPEMIG for their continuous support to develop research and for their financial assistance.

ABSTRACT

Nowadays, the transition from conventional fossil fuel based and centralized energy generation to distributed renewables is increasing rapidly, due to the environmental concerns and political incentives. Wind and solar power generation offer carbon dioxide neutral electricity but also present some integration difficulties for energy system operators and planners due to intermittent power output. A promising way of dealing with the intermittency from renewables is energy storage. Many types of energy storage have been under development and study. Therefore, a battery energy storage system has been implemented mainly in residential applications to utility power grids. Battery energy storage can allow higher amounts of renewable electricity generation to be integrated by smoothening power output, and time shifting generated energy to follow demand and increase hosting capacities through peak shaving. Power quality related issues due to intermittency can be mitigated by controlling the storage's charging patterns to respond to grid variables. For optimal utilization and maximum storage value, several applications should be within the operational repertoire of the storage unit. Other applications, including arbitrage, grid investment deferral, and load following, are discussed. This thesis proposes a study and analysis of the Conti-Varlet approach or stretched-thread method (STM) a powerful graphical based technique used to partial flow regularization for hydropower plants to provide auxiliary service regularization considering a battery energy storage system (BESS). The proposal is maintaining the power more stable and constant as possible, mitigating the PV intermittence. A one-year analysis is performed for each BESS size, ranging from 10% to 90%. A cost for each scenario and an optimal BESS is presented to reduce the disutility. The changing of the consumption costs is defined as disutility.

Index Terms — Battery, Conti-Varlet, disutility, energy storage, photovoltaic system, renewable energy.

SUMMARY

LIST OF FIGURES

LIST OF TABLES

LIST OF ABBREVIATIONS

AC	Alternating Current
ARES	Advanced Rail Energy Storage
BESS	Battery Energy Storage System
CAES	Compressed Air Energy Storage
CES	Cryogenic Energy Storage
DC	Direct Current
DG	Distributed Generation
DHI	Diffuse Horizontal Irradiance
DNI	Direct Nominal Irradiance
DOD	Depth of Discharge
ESS	Energy Storage System
FACTS	Flexible Alternate Current Transmission System
FES	Flywheel Energy Storage
GAMS	General Algebraic Modeling System
GHI	Global Horizontal Irradiance
HES	Hydrogen Energy Storage
JET	Join European Torus
LINDO	Linear Interactive, and Discrete Optimizer
MILP	Mixed Integer Linear Programming
MIP	Mixed Integer Programming
MME	Ministry of Mines and Energy
MPPT	Maximum Power Point Track
NOCT	Nominal Operating Cell Temperature
PCM	Phase change materials
PHS	Pumped Hydro System
PV	Photovoltaic
SCES	Supercapacitor Energy Storage
SMES	Superconducting Magnetic Energy Storage
SOC	State of Charge
STM	Stretched-Thread Method
TES	Thermal Energy Storage

TOU	Time of Use Tariff
UK	United Kingdom
UPS	Uninterrupted Power Supply
USA	United States of America
WEC	World Energy Council

CHAPTER 1 - INTRODUCTION

With the continuous increase in the consumption of electric energy in the world and the use of exhaustible resources, new forms of power generation have been developed for a reduction of environmental impact and to meet the increasing demand of electrical energy. These issues require development in order to optimize energy use and minimize fuel consumption and toxic emissions. Various alternatives to the use of fossil fuels have been proposed so as to achieve such sustainable energy systems. Renewable energy generation and an energy storage system such as sources of renewable energy, energy from the wind and the sun, for example, are the sought solution [1].

In many countries, the use of renewable energy has been growing exponentially since the end of the last decade. By 2017, the total worldwide installed capacity of photovoltaic was 402 GW. China continued to lead the photovoltaic generation capacity of 131.1 GW, followed by United States (USA) with 51.5 GW, Japan with 49.8 GW and Germany with 43 GW as shown in Figure 1 [2]. According to data from the Ministry of Mines and Energy (MME), at the end of 2017, Brazil was among thirty countries with an installed capacity higher than 1 GW, thus putting it in the top ten countries that add more PV plants in the energetic matrix [3].

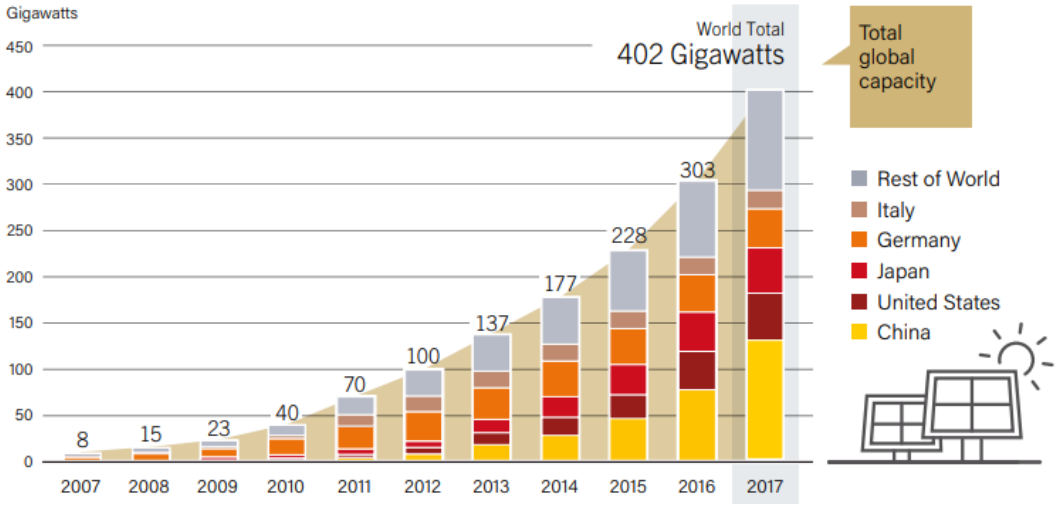

Figure 1 - Solar installed capacity by country.
Source: [2].

Solar potential is higher in Brazil than in other countries, specifically in the northeast region which presents the most significant values of global solar irradiance. Also, this area

provides favorable climate conditions throughout the year. The average Brazilian irradiance is between 1,200 and 2,400 kWh/m²/year which is higher than average values found in Europe [4] [5].

According to the 2018 Renewable Global Status Report (REN21), wind power generation has reached 539 GW of clean, renewable power that was installed in the world in 2017. China, for the ninth consecutive year, led the wind power generation capacity with 188.4 GW, followed by the European Union with 168.7 GW, North America (United States with 89 GW and Canada with 12.2 GW) [2]. Brazil continued among the top ten with 12.8 GW. The wind market can be divided into onshore rates with an installed capacity of 520 GW, and offshore rates with around 18.8 GW installed. Figure 2 shows the wind installed capacity in the world.

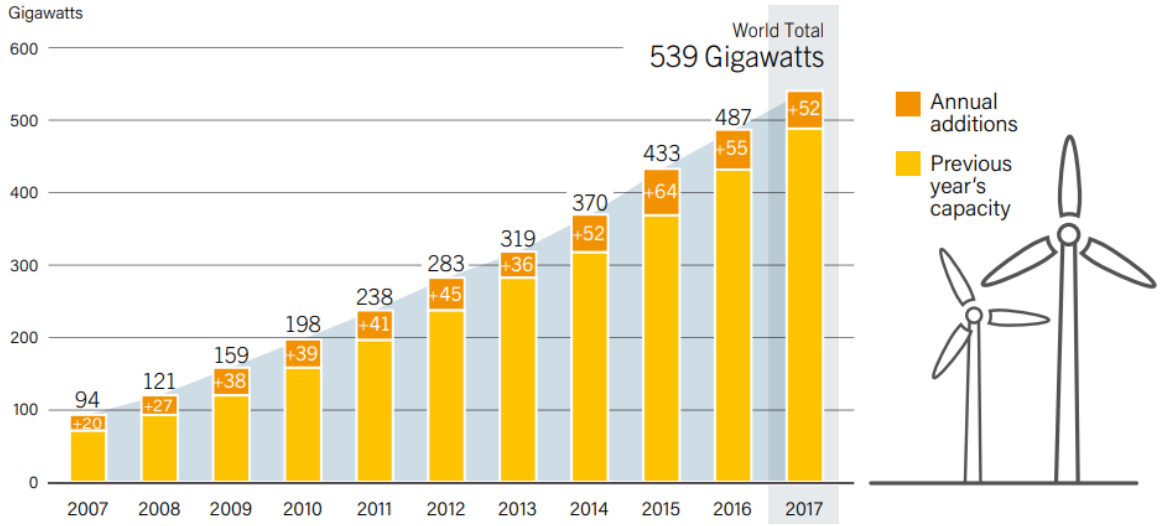

Figure 2 - Wind installed capacity in the world.
Source: [2].

These sources of generation are being generated locally (distributed generation) and are directly connected to the distribution system despite the power grid system, with exception to the wind power generation. As a consequence, less controllable energy generation, the need for bidirectional power flows and the transformation of ordinary consumers to a new term “prosumers” have resulted [6]. The prosumers are local households that are qualified as producers and consumers of electricity and that have a decentralized production unit (DPU) [7]. However, the availability of variable resources often does not positively correlate with the power demand. The development and injection of new loads on the power system network imply possible problems with system stability. As a result, the use of energy storage systems

(ESS), along with renewable sources, becomes indispensable for generation operation and control.

The use of ESS makes it possible to manage the reliability and resilience of variable generation systems and improve the functionality of micro-networks as well as smart grids. Figure 3 shows the energy storage installations in the world by the type of technology over time while excluding the pumped hydro storage (PHS). Various storage technologies have had significant development over the last decade, such as compressed air, flywheels, and liquid air energy storage. However, the PHS is the most developed and widely applied type of ESS. For the year 2017, the PHS has 153 GW of storage capacity installed in the world followed distantly by thermal storage with 2.3 GW, and then by batteries with 2.3 and electro-mechanical storage of around 1.3 GW [2]. Figure 4 shows the new deployed storage power capacity across global markets for the year 2017.

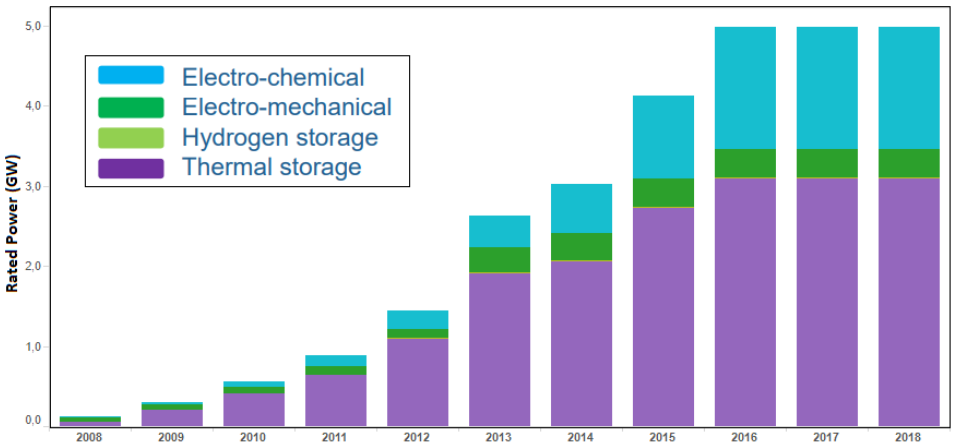

Figure 3 - Global energy storage installations, excluding PHS.
Source: [8].

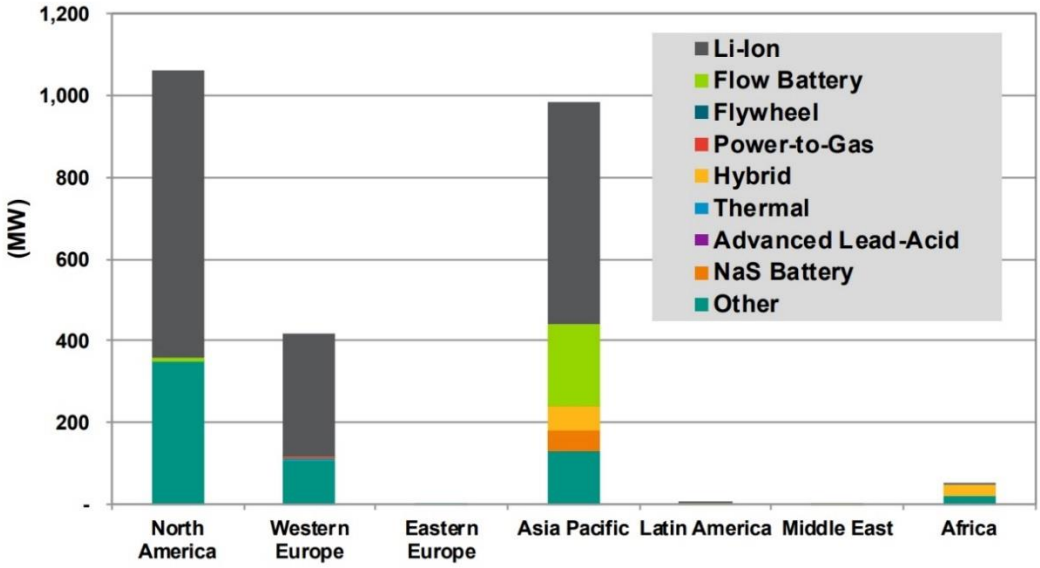

Figure 4 - ESS Power capacity by technology and region.
Source: [8].

The electric energy in an alternating current (AC) cannot be stored. Thus after being generated, it is converted into another type of energy to be stored, electrochemical, kinetic or potential energy, allowing a movement of electric energy over time since this energy process enables it to be generated and consumed at different times [9]. In general terms, the electricity to be dispatched in periods of high demand is low generation which is used in periods of high consumption or functioning as a backup in cases where the central generation becomes inaccessible [10]. Also, it helps to reduce the usage of exhaustible fossil fuels, cutting greenhouse gas emissions that are associated with global warming. As a result, energy storage systems (ESS) have recently attracted the attention of governments, stakeholders, researchers, and investors as they may be used to improve the overall performance of the energy supply chain.

With the increased dissemination of distributed generation (DG) on the grid, some impacts will occur in the system. Some examples of these are bidirectional power flow, voltage profile and utility equipment [11]. Considering a photovoltaic system (PV) farm on a cloudy day, the produced generation goes down, and as a consequence, the voltage delivered to the load is reduced. In other words, the system will present faster voltage variations. To minimize this contingency, an ESS can be used.

The irradiance provided by the sun and the speed of wind are random in the same way that water flows in a river, though it is more predictable. Nevertheless, there are methods based on historical data that can be used to design and predict the volume flow of a dam which result

in a flow regularization. Due to the irradiation intermittence, the use of energy storage becomes necessary in order to store the power that is not used by the consumers. Besides the technology and dimension of the ESS, the primary goal is to provide as much continuous power as possible, even with the irradiance drawback.

Over the past century, a powerful graphing technique was developed using the stretched-thread method (STM), or Conti-Varlet technique. This approach was mainly used to flow regularization in hydropower plants [12]. The term regularization used in this research is a synonym of regulation. In this context, a new approach to the Conti-Varlet technique is presented and applied in a PV system in order to regulate the power available in the BESS. The power regularization is a process that has the objective of improving the PV power use as well as choosing the optimal BESS that reduces the disutility (cost for changing consumption).

1.1 Thesis Outline

This thesis is made up of 6 chapters. In the present chapter, an introduction is made that shows the general scenario in which ESS technologies are applied.

Chapter 2 - Energy Storage Technologies: In this chapter, we discuss the state of the art of various energy storage technologies, their applications, as well as economic and market factors related to them.

Chapter 3 – Flow Regularization Review: In this chapter, a review of the flow regularization is made along with with its application and the development of a new application on an energy storage system.

Chapter 4 – BESS Optimal Sizing Review: A review of optimization methods applied in the energy storage system is made.

Chapter 5 – Problem Outline and Variables: This chapter presents a brief solar data theory and a BESS optimization model to reduce the costs of energy purchased from the utility (disutility).

Chapter 6 – Results and Analysis: This chapter describes the methodology used and the results obtained.

Chapter 7 – Conclusions: In the last chapter, remarks, conclusions, and future research suggestions are presented.

1.2 Research Objectives

Photovoltaic power is obtained by the conversion of sunlight directly into electricity. In 1954, Alexander Graham Bell discovered the PV effect, which is the process of converting light (protons) into electricity. Solar cells are made from silicon, usually flat-plane, and are generally the most efficient. The sunlight absorbed by solar cells allows the electrons to be released from the movement of atoms. The interaction between the photons released from the sun and the particles released from the solar cell create the direct current [13].

The PV cells are typically connected through a series or in a parallel way and mounted on a frame called a module to obtain the desired output voltage. The PV modules can be wired together to form a cluster which can then be scaled up or down in order to produce the amount of power that is necessary [14].

The main disadvantage of this generation type is its dependency on the sun which causes intermittent power generation. The intermittent characteristic is very common in renewable sources. Additionally, the integration within the grid has various limitations because of its weather dependency and the component constraint [15]. Therefore, it becomes a vital factor in the use of ESS along with renewable sources for generation, operation and grid planning.

On a grid with an ESS, optimal sizing should be performed. The oversized BESS tends to be economically unattractive while an undersized BESS may not render the desired benefits. In this way, an optimal size for the storage system should be found in which the reduction of energy purchased from the utility due to the addition of the BESS is more substantial than the BESS investment costs imposed by the storage.

The normal strategy used is to sell electricity when the regulated power is higher than the load demand and buy energy from the utility when the regulated power is less than the load demand. The price is calculated from each regularization scenario, and the results will be compared thereby determining what amount of the battery will result in the lowest disutility.

1.2.1 Methodology

The study at hand is based on a new approach to the Conti-Varlet method, a well-known technique applied to hydropower plants used in PV system integrated with a BESS.

Based on the elaboration of the problem, the objectives of the study are defined, and the literature review is carried out which consists of the explanation of the following three main

points: characteristics of the energy storage technologies, flow regularization methods, and BESS optimal sizing.

Once the theoretical framework is finished, the problem logic is developed which is then implemented through a mathematical optimization model in order to size an optimal BESS size to reduce the disutility.

1.3 Objectives

The primary objective of this thesis is shown via a simulation model to size and analyze a battery energy storage system using the Conti-Varlet technique in order to act as a regulatory reserve and therefore reduce the disutility.

1.3.1 Sub-Objectives

The sub-objectives of this thesis are:

1. Provide a study of energy storage technologies, approaching the operation principle, application, advantages, and disadvantages;
2. Show the use of the Conti-Varlet technique.
3. Complete tests in the model proposed and analyze the results.

CHAPTER 2 - ENERGY STORAGE SYSTEMS: APPLICATION AND TECHNOLOGIES

Energy storage was not recently developed but rather discovered more than two centuries ago when Luigi Aloisio Galvani discovered bioelectricity through an experience involving a frog. Around the year 1800, Alessandro Volta invented the modern battery, combining different metals that are separated by salt or some kind of acidic solution. However, it was only in 1836 that they were used in telegraph networks. In 1880, lead-acid batteries were used to empower private night loads in New York in areas with a direct current (DC) system. The first large-scale storage system was built in 1929 as a 31 MW pumped storage at Rocky River Power Plant by Connecticut Light & Power [15].

Some ESS technologies store energy in the direct current (DC) form, making the use of a DC/AC converter necessary. This is true in the case of batteries, flywheels, and supercapacitors, for example. Two significant factors characterize the application of an energy storage technology system. The first of these is the amount of energy that can be stored, which is a characteristic of the storage device itself. Second is the rate at which energy can be transferred into or out of the storage device. This mainly depends on the peak power rating of the power conversion unit but is also impacted by the response rate of the storage device itself [16].

This chapter provides an overview of potential applications of storage systems. Technical and economic characteristics of each storage technology, including power rating, typical discharge times, investment and operation costs, efficiency, response time, and lifetime are also presented.

2.1 ESS Applications

The ESS provides benefits to grid operations from distributed generation-to-utility scale installations. A significant addendum is that which achieves the benefits provided by the ESS. Likewise, the best storage technology should be wisely selected for its application. In Figure 5, the groups of technologies are presented according to their discharge time, power and application. Several of these services provided are described below [15] [16] [17]:

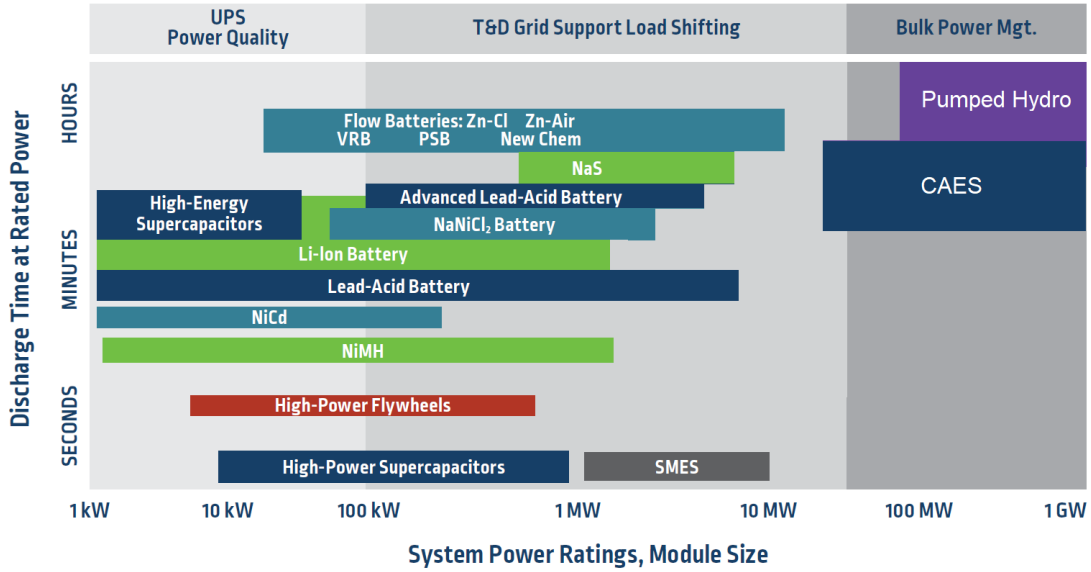

Figure 5 - Comparison of energy storage technologies.
Source: [15].

2.1.1 Bulk Energy Services

Bulk energy storage involves shifting the energy production of current generators that utilities that can buy the energy from a low price (off-peak) and sell it for a high price (on-peak). With the variability of renewable generation, especially in PV and wind generation, increases can affect the wholesale market price volatility. Prices tend to go down when generation is high and they tend to get recovered when production decreases.

Electric energy time-shift involves many possible transactions with economic merit based on the differences between the cost to purchase, store, and discharge energy, and the benefits derived from them when the energy is discharged. Also, the time of day and season can be considered as a bulk service. The possibility of storing energy provided by renewable sources in seasons and diurnal differences is very beneficial to the system.

2.1.2 Ancillary Services

Ancillary services, by definition, are services that support the transmission of electricity from its generation site to the customer or that help maintain its usability throughout the system. Energy storage technologies are individually appropriate in order to provide ancillary services, which are currently being performed by generators that are not designed for this purpose.

Moreover, the provision of ancillary services impairs the primary function of traditional power generation assets by requiring that they operate at suboptimal levels in order to respond to changes in the grid. Energy storage, on the other hand, offers responsive technologies that can accommodate the need for frequent but relatively short discharges [18]. Some of the benefits provided are described below.

2.1.2.1 Regulation

Frequency regulation (area regulation) is an ancillary service that entails moment-to-moment reconciliation of the differences between electric supply (power) and electric demand. The primary purpose of frequency regulation is to maintain the stability and accuracy of the system-wide alternating current (AC) frequency as shown in Figure 6 within a given "control area."

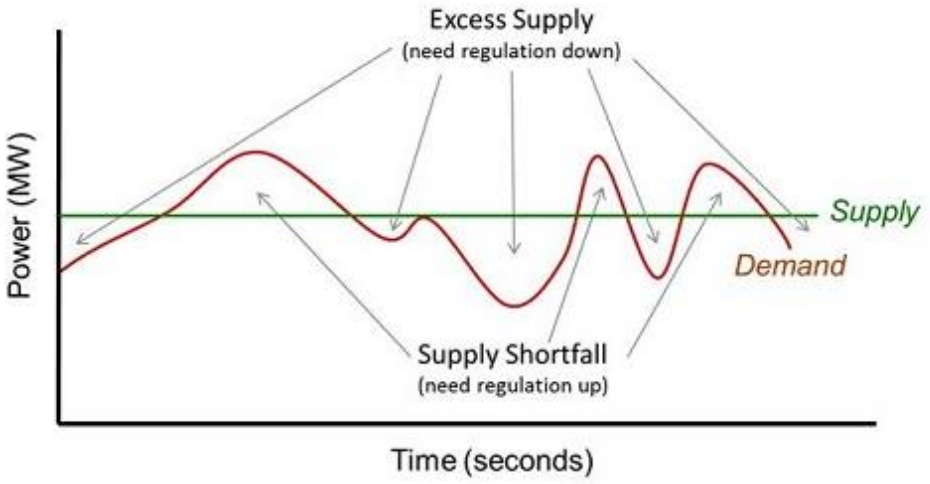

Figure 6 - Frequency Regulation.
Source: [19].

As shown in Figure 6, when supply momentarily exceeds demand (excess supply), frequency regulation down is needed to offset the discrepancy. Conversely, when supply is momentarily below demand (supply shortfall), frequency regulation up is required in order to compensate for the difference.

When the ESS provides down-regulation by charging, it absorbs energy from the grid, making for a situation in which the storage operator must then pay for that energy.

2.1.2.2 Black-Start

Black-Start provides an active reserve of energy and power to the grid after a system failure. A black-start unit can also provide energy to help other units restart and provide a reference frequency for synchronization.

2.1.2.3 Spinning, Non-Spinning, and Supplemental Reserves

For a grid operation, a reserve capacity is necessary that can be used when some portion of the primary electric source becomes unavailable. The reserves can be categorized as follows:

- Spinning reserve: In this case, this is the unloaded generation that is synchronized and ready to supply the demand. The response time is 10 minutes to compensate for generation or transmission outages.
- Non-spinning reserve: Fundamentally consists of a generation that is offline but can be brought online within 10 to 30 minutes.
- Supplemental reserve: Generation that can pick up a load within one hour. Supplemental reserve works as a backup for spinning and non-spinning reserves, and supplemental reserve capacity is not synchronized with grid frequency.

2.1.2.4 Power Quality and Stability

Energy storage can be used to assist in a general class of services referred to as power quality and stability. Voltage spikes, sags, momentary outages, and harmonics can be classified as power quality issues. Storage devices are often used at customer load sites to buffer sensitive equipment against power quality problems. Electric power systems can also experience oscillations of frequency and voltage. Unless dampened, these disturbances can limit the ability of utilities to transmit power and affect the stability and reliability of the entire system. System stability requires response times of less than a second and can be met by a variety of devices, including fast-responding energy storage [20].

2.1.3 Transmission and Distribution

Storage can act as an alternative or supplement to new transmission and distribution. Energy can be stored during off-peak periods when the distribution system is lightly loaded and discharged during peak periods when the system may otherwise be overloaded. Energy storage can also reduce the high line-loss rates that occur during peak demand.

2.2 ESS Characteristics

The EES technologies are divided into two major groups: systems for energy applications (for medium and long-term duration needs) and power applications (for short and very short-term duration needs). Each type of technology has its strengths, limitations, and appropriateness for their large and diverse set of applications [21] [22]. However, non-conventional technologies are in the research and developmental phase, such as Advanced Rail Energy Storage (ARES), which store the energy employing electric locomotives [23]. Other factors that influence the choice of ESS technology for a particular application include response time, discharge frequency, depth of discharge, efficiency, service life and system costs.

2.2.1 Technical-economic characteristics of ESSs

Power capacity is the rate of discharge of the storage devices. It is measured in kilowatts (kW) or megawatts (MW). The power capacity of an ESS is its nameplate power rating under normal operating conditions. Such a power rating also represents the storage device maximum power output under normal operational conditions. This feature is often referred to as the storage peak power rating or pulse power rating, which is usually several times greater than the standard power rating. This power rating is necessary for circumstances involving an urgent need for relatively high-power output within quite short durations. However, discharging at a higher rate will gradually reduce storage efficiency and the storage device will lose its life more easily (compared to damage incurred at the normal discharge rate) [24].

Another significant characteristic of a storage system is the discharge duration which is expressed in units of time that ranges from seconds to hours. Discharge duration is the amount of time that the storage plant can discharge at its rated power without being recharged. This

characteristic is also represented by the energy capacity of the ESSs, where energy capacity, measured in kilowatt-hours (kWh) or megawatt-hours (MWh), is defined as the *power capacity x discharge duration*. For instance, an ESS with a power capacity of 1 MW and energy capacity of 5 MWh can deliver 1 MW in 5 hours when fully charged [15].

2.2.2 Depth of Discharge, Frequency of Discharge, and Response Time

The depth of discharge is the percentage of power discharged relative to its full capacity before the storage is recharged. Some technologies are sensitive to the depth of discharge. Deep discharge of some electrochemical batteries reduces their life expectancy and may cause physical damage to the battery cells. Other technologies operate best under full or 100% depth of discharge [25].

The frequency of discharge is how often power will be discharged from storage technology. Some applications only require infrequent discharge (spinning reserve, for example) while others are cycled continuously.

Response time is how quickly a storage technology can be brought online and start discharging its energy. Most storage technologies have a response time of several seconds or less.

2.2.3 Service Life

The life cycle is the approximate number of charge and discharge cycles that a particular energy storage device can undergo before it fails. For many energy storage devices, cycling introduces structural, mechanical and thermal stresses which form the life-limiting factor for the device [25] [26].

For some energy storage technologies such as electrochemical batteries, the life cycle depends on how deeply the battery is discharged from a full charge. The deeper the average discharge, the more the battery will be exercised and the shorter its life will be.

Three major factors affect its lifetime and whenever one of them reaches its limit, the energy storage system should be replaced.

- The calendar lifetime (years): after a period (years) of installation, depending on the technology, the energy storage may not operate efficiently even though it may not have operated frequently.
- Number of cycles (cycles): when the number of charging/discharging cycles reaches its maximum, the energy storage system should be replaced. This factor is critical in applications requiring frequent shallow charge/discharge cycles.
- Total discharged energy (kWh or MWh): in applications that require deep charging and discharging cycles, the total discharged energy determines the lifetime of energy storage.

2.2.4 Roundtrip Efficiency

There are several ways to measure the efficiency of an energy storage device, but in the utility industry, the most commonly used one is the AC round-trip efficiency measure. AC round-trip efficiency is determined as the AC energy input to the AC energy output ratio. Self-discharge loss during the storage operation is not included. For example, a 10 MW/50 MWh battery system may require a 60 MWh energy input to charge the empty storage device fully. The system can then be discharged to deliver 50 MWh. The efficiency of this system would be 50MWh/60 MWh or 83.3%.

Generally, ESSs can be divided into three groups based on the round-trip efficiency [8]:

- Very high efficiency: the ESSs have very high efficiency, *i.e.*, more than 90%. Some examples of this group include Superconducting Magnetic Energy Storage (SMES), flywheel, super-capacitor, and Li-ion battery.
- High efficiency: the ESSs have an efficiency of 60-90%. For example, Pumped Hydro Storage, Compressed Air Energy Storage, batteries (except for Li-ion), flow batteries and conventional capacitors.
- Low efficiency: the ESSs have an efficiency lower than 60%. Hydrogen, Metal-Air, solar fuel and Thermal Energy Storage belong to this group.

There may be a trade-off between capital cost and roundtrip efficiency when choosing a storage technology. For instance, storage technology with a low capital cost but a low roundtrip efficiency may be competitive with a high price and high roundtrip efficiency technology. The efficiency of ESSs is affected by several different factors. For most energy

storage technologies, energy is lost during the process of charging and discharging. Energy may also be lost while the device is not in use. These losses are called standby losses. Standby losses are a measure of efficiency that compares how much of the energy used to charge a storage device is lost before discharging. Moreover, if the storage system does not operate at the same voltage as the system, losses arise since a step-up/step-down transformer must be used. ESSs that store only DC power must include a charger and an inverter to convert AC power to DC power for storage, and then back again for delivery; these power electronics also generate losses. Some technologies have other intrinsic losses such as the thermodynamic losses in batteries. Efficiency can also be affected by environmental conditions like temperature [27].

2.2.5 System Cost

The cost of an ESS follows two metrics: cost per unit power (U$/kW) and cost per unit energy (U$/kWh). Cost per unit power is used in the same manner that other capital investments in the utility industry are usually described. It is defined as the cost per unit of rated power and can be used with equipment cost (cost of the installed device), installation cost, or life-cycle cost. Price per unit energy, U$/kWh, describes the cost per unit of energy storage capacity.

2.3 ESS Technologies

The most widely used approach for classifying storage systems is that according to the form of the energy stored in the system, as depicted in Figure 7. In general, it is based on the way that energy is stored in the system which can be mechanical (pumped hydroelectric storage, compressed air energy storage and flywheels), electrochemical (conventional rechargeable batteries and flow batteries), electrical (capacitors, super-capacitors and superconducting magnetic energy storage), thermochemical (solar fuels), chemical (hydrogen storage with fuel cells) or thermal energy storage (sensitive heat storage and latent heat storage).

Nowadays, batteries are the most widespread electrical energy storage technology. Analysts expect advancements in ESS to occur with the maturation of new technologies, such as metal-air batteries, and the application of new materials and designs of proven technologies like lead-acid [28]. As an example, Tesla Inc. installed the largest Lithium-ion battery energy

storage system (BESS) in the world in southern Australia in 2017 with 100MW of capacity. This system works as a backup to the power system.

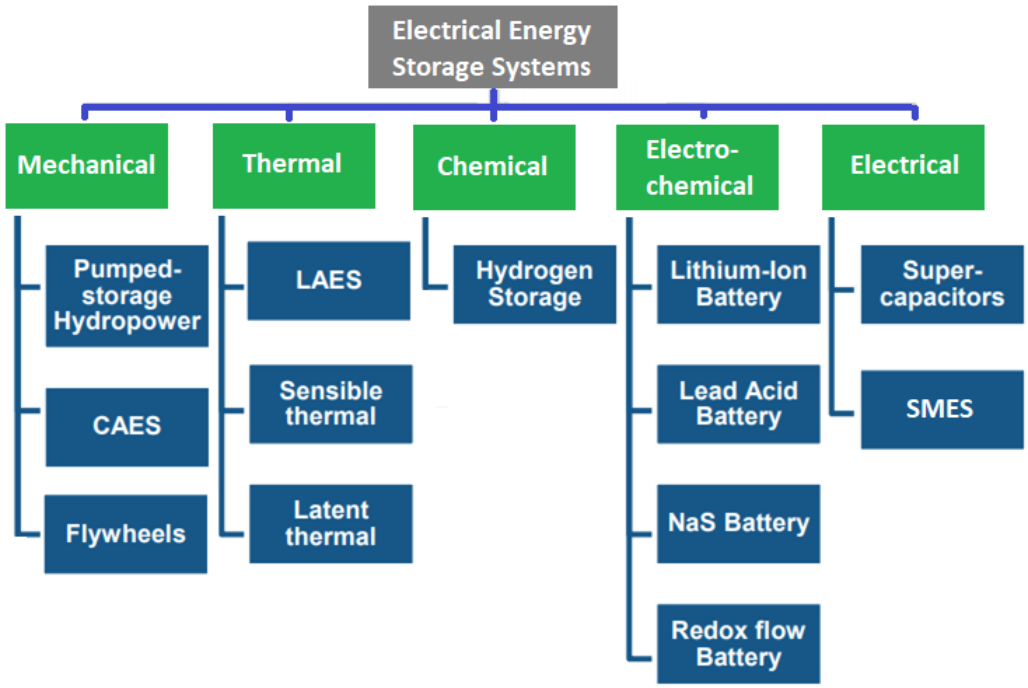

Figure 7 - Classification of energy storage technologies according to energy form.
Source: [29].

2.3.1 Mechanical Storage

At the present time, electrical energy can be stored in different forms, such as mechanical energy. Mechanical storage exchanges its stored energy with the power grid in the form of kinetic or potential energy. The most common mechanical energy storage technologies are pumped hydro storage (PHS), compressed air energy storage (CAES) and flywheel energy storage (FES) [21].

2.3.1.1 Pumped Hydro Storage

PHS systems are among the oldest and most widely used energy storage options and therefore, are fully commercialized. In addition to this, they are currently the only existent type of commercially proven, large-scale, economically viable (>100 MW) energy storage

technology. The fundamental principle of this storage type is storing electric energy in the form of hydraulic potential energy. Water is stored in an upper reservoir and is processed in a turbine to recover its potential energy in the form of mechanical energy [30]. Figure 8 shows a simplified schematic of a PHS. During its off-peak, water is pumped into a high peak reservoir, and in peak hours, water is released back to the lower level reservoir. The turbine drives the electric machine in order to generate electricity. The amount of energy stored depends on the volume of water stored in the reservoir and the height difference between both reservoirs. Rated power depends on the flow rate of water through the turbine and its pressure. The generated energy is defined by the expression below.

$$E_{PHS} = \rho \cdot g \cdot H \cdot V \quad (1)$$

Where E_{PHS} is the stored energy (J), ρ is the density of the water equal to 1000 kg/m³, g is the acceleration due to gravity equal to 9.8 m/s², H is the height of the waterfall (m), and V is the volume of water stored in the upper reservoir.

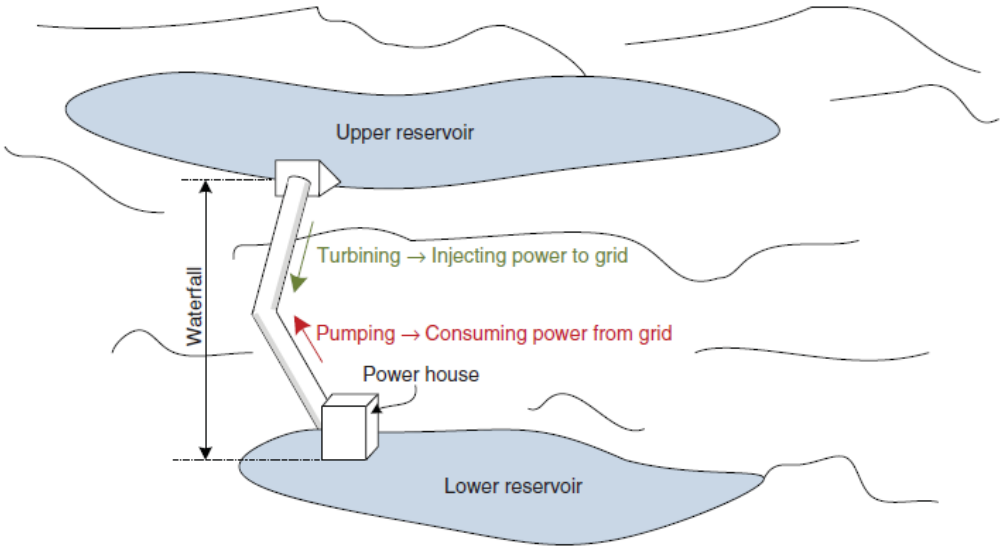

Figure 8 - Simplified schematic of PHS.
Source: [6].

PHS had a large energy capacity of over 150 GW installed capacity in the year 2016, representing around 99% of storage capacity in the world and contributes up to 3% of global generation [31]. Bath County PHS, in Virginia, USA, is the worldwide leader with a generation capacity of 3003 MW and discharge time of 10 hours at rated power, but China is expanding quickly and expected to surpass the US. China has two large PHS stations, Huizhou and

Guangzhou, both of which are located in the Guangdong province and have respective capacities of 2448 MW and 2400 MW [32].

The advantages of such a system are its long life, established technology, enormous installed capacity, and practically unlimited life cycle. By storing electricity, PHS facilities can protect the power system from an outage. The main disadvantage of PHS technology is that it requires large dams or reservoirs for water, high investment costs, low energy density, a longer time for construction as well as being associated with some environmental issues [33] [9].

2.3.1.2 Compressed Air Energy Storage

Compressed air energy storage energy (CAES) is another type of energy storage technology which can provide a power output of over 100 MW with a single unit. A representation of a CAES plant is presented in Figure 9.

The energy is stored in the form of compressed air in an underground storage cave at pressures between 40-70 bars. An additional possibility is to store the air in above-ground tanks. The air is additionally mixed with natural gas and combusted for increased efficiency. When energy needs to be injected into the grid, the compressed air is drawn from the storage cave, heated, and then expanded into a set of high and low-pressure gas turbines which then convert most of the compressed air energy into rotational kinetic energy. Next, the rotational energy is converted into electrical energy in a generator. While driving the electrical generators, the turbine exhaust is used to heat the air in the cavern [6].

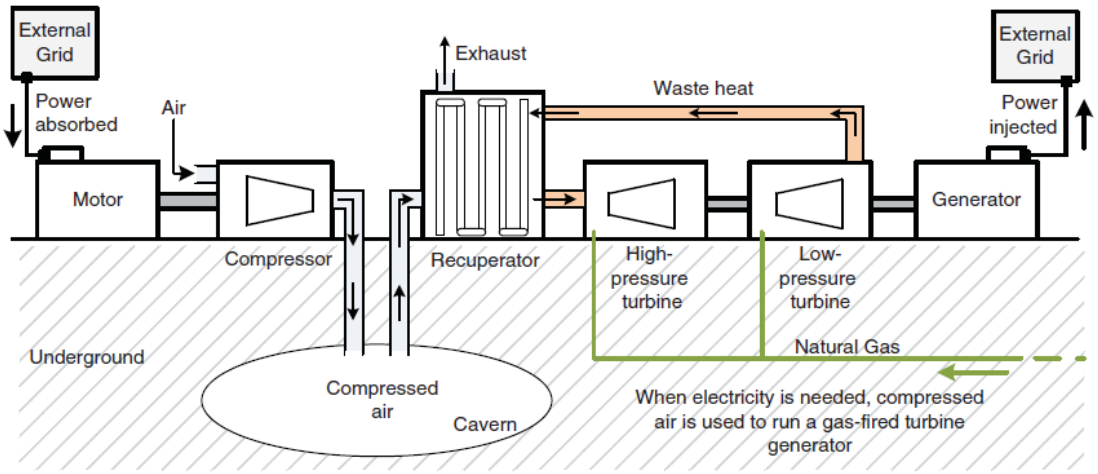

Figure 9 - Schematic of large-scale diabatic CAES Plant.
Source: [15].

The most recent technologies that have been applied in CAES are focused on adiabatic systems. In an adiabatic CAES system, the heat generated during the compression process is stored. During its discharge phase, the stored heat is used to heat up the air while expanding. Currently, there is only one adiabatic CAES of scale in operation. However, it is a demonstration plant used to test a novel adiabatic CAES located in an abandoned tunnel in the Swiss Alps with a rated power of 500 kW [34].

A conventional CAES system separates the compression and expansion cycles of a traditional peaking gas turbine into two decoupled processes and stores the electrical energy in the form of elastic potential energy of compressed air [27] [35]. During low demand, energy is stored by compressing air up to 100 bars at near-ambient temperatures into a sealed space, typically an underground cavern (charging operation mode, with the motor driving a compressor). When the power demand is high and stored energy is required, compressed air is drawn from the storage chamber, heated up by burning conventional fuel (or biofuel) and then expanded through a high-pressure turbine which captures some of the energy in the compressed air (discharging operation mode). The air is then mixed with fuel and combusted with the exhaust expanded through a low-pressure turbine. Both the high and low-pressure turbines are connected to a generator to produce electricity. The waste heat of the exhaust is potentially captured via a heat exchanger or recuperator before being released [21].

There are two operating first-generation CAES systems in the world: one in Germany that uses salt domes as the storage caverns and that runs on a daily cycle with 8 hours of compressed air charging and 2 hours of operation at a rated power of 320 MW, and one in the state of Alabama, USA that has 110 MW of capacity and can operate for up to 26h at full power with compressed air that is stored in a salt cavern. Both CAES plants have steadily shown good performances with 91.2% and 99.5% starting and running reliabilities [21]. As a PHS system, a CAES is characterized by an enormous power and energy capacity, an extended service lifespan and a low unit cost and low cost per kW.

CAES systems can be built to have a small to large scale of capacities that provide the moderate speed of responses and good partial-load performance. The practical uses of large-scale CAES plants involve grid applications for load shifting, peak shaving, and frequency and voltage control.

The main advantages are that they are relatively low cost for the energy storage (caverns), they leave a small footprint on the surface, they have long life in the air reservoir and in the power systems. The main barrier in employing large-scale CAES plants are certain

geological restrictions necessary, high investment costs, high self-discharge of the thermal storage and long return investment (>30 years) [33].

2.3.1.3 Flywheel Energy Storage

The advanced flywheel energy storage (FES) system is composed of five primary components: a flywheel, a group of bearings, reversible electrical motor/generator, a power electronic unit and a vacuum chamber, as shown in Figure 10. FES systems use electricity to accelerate or decelerate the flywheel; that is, the stored energy is transferred to or from the flywheel through an integrated motor/generator. The energy is stored in the form of the angular momentum of a spinning mass called a rotor [36].

The stored energy depends on the moment of inertia of the rotor and the square of the rotational velocity of the flywheel. The moment of inertia (I) depends on the radius, mass, and length of the rotor. The energy is transferred to the flywheel when the machine operates as a motor, charging the energy storage device. When the stored energy is required, the generator converts the stored kinetic energy into electricity through the power electronics interface [16].

Typically, the FES has the capacity to store between 0.5 kWh and 10 kWh. The largest commercially available systems of this type are in the 2 kWh to the 6kWh range with plans for 25 kWh. All energy generated by flywheels today is used in DC systems [15]. The FES can be charged relatively quickly. Nowadays, the FES is in shorter energy duration systems and is not attractive for large-scale grid support services that require a considerable amount of energy (kWh-MWh). FES systems can be classified in two types: conventional low speed which uses steel as the flywheel material and rotates below 10000 rpm and high-speed units which use advanced high-strength composite materials for the flywheel, such as carbon-fiber and rotates up to 100,000 rpm [37].

The FES generally exhibits an excellent life cycle in comparison to other energy storage systems with an estimated life cycle life of 100,000 full charge-discharge cycles with full charge-discharge (more than 12 years of life) [38]. In spite of this, FES has a power density of 5 to 10 times that of batteries. In other words, it requires much less space to store a comparable amount of power [16]. The total energy stored by a flywheel system is dependent on the size and speed of the rotor as stated by equation (2), while the power rating is dependent on the motor/generator.

$$E_{FESS} = \frac{1}{2} \cdot J_F \cdot \omega_{mF}^2 \quad (2)$$

Where E_{FESS} is the energy stored by the FES (J), J_F is the moment of inertia (kg·m²) of the FESS and ω_{mF}^2 is the rotor mechanical speed (rad/s).

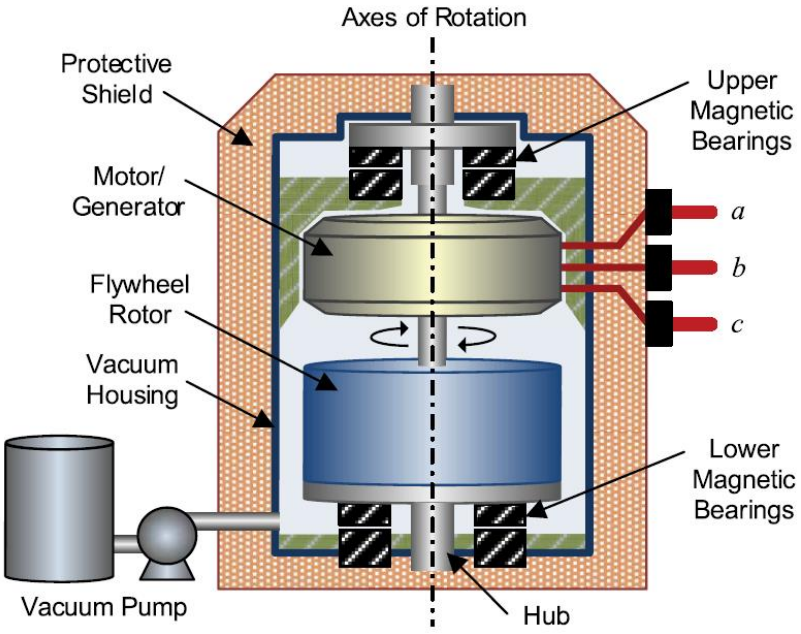

Figure 10 - Flywheel system.
Source: [21].

There are many FES systems in operation worldwide that have an installed capacity exceeding 940 MW [32]. The three largest operational utility-scale FES facilities are: the Joint European Torus (JET) Fusion FES facility in Culham, Oxfordshire, United Kingdon, which is the largest flywheel energy storage station in the world. Installed in 2006, it has a power capacity of 400 MW and a discharge time of around 30 seconds at rated power (12000 MJ). The second biggest FES system is the Max Planck Institute ASDEX-Upgrade Pulsed Power Supply System which was installed in 1981 in Garching bei München, Bavaria, Germany, with a power capacity of 387 MW and a discharge time of around 12 s at rated power (4700 MJ). Finally, the Institute of Plasma Physics (IPP) has a Flywheel System that was installed in 2008 in Prague, Czech Republic and has a power capacity of 70 MW and a discharge time around 5s at rated power (350 MJ) [21].

The main advantages of the FES are the fast charge capability, low maintenance requirements and long life. Its weaknesses include its low density, cooling system for superconducting bearings and very high self-discharge [33].

2.3.2 Electrical Storage

The most direct way of storing electrical energy is in the same way as electrical energy itself. The electrical energy storage mainly contains supercapacitor energy storage (SCES) and superconducting magnetic energy storage (SMES).

2.3.2.1 Supercapacitor Energy Storage

Capacitors store electrical energy in the electrostatic field produced between two conducting plates (electrodes) separated by a thin layer of an insulator (dielectric) when a constant DC voltage is applied within them. Supercapacitors are also denominated double-layer capacitors or ultra-capacitors, as shown in Figure 11. A dielectric material decides the maximum operating voltage of the capacitor.

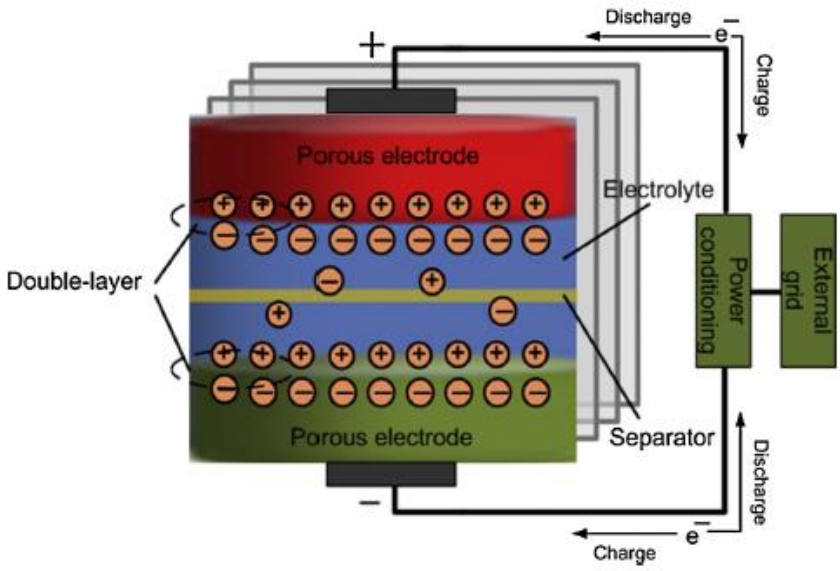

Figure 11 - Diagram of a supercapacitor.
Source: [36].

The capacitor has a high power density, shorter charging time, lower capacity, lower energy density and high energy dissipation. A supercapacitor is also recognized by the name called electric double-layer capacitor or ultra-capacitor. It is a relatively modern technology in the field of short-term energy storage systems for grid applications [36]. The first high-power

supercapacitor with low internal resistance was developed in the early 1980s in the US for portable military applications [39].

In comparison to conventional capacitors, the supercapacitors have significantly larger electrode surface areas coupled with a thinner electrical layer's thickness of only a few molecular diameters. These attributes mean that supercapacitors have higher capacitances and therefore higher energy densities than conventional capacitors. The current carrying capability of the supercapacitors is exceptionally high since it is directly proportional to the surface area of the electrodes. The power density is extremely high, reaching values of 10,000 W/kg, which is more than batteries can achieve. However, due to the low energy density, this high amount of power will only be available for a quick duration [36]. The amount of energy stored as static charge on the surfaces between the electrolyte and two conductor electrodes in a supercapacitor unit is given by (3):

$$E_{SCES} = \frac{1}{2} \cdot C_S \cdot V^2 \tag{3}$$

Where E_{SCES} is the energy stored by the supercapacitor system (J), C_S is the double-layer capacitance (F) of the supercapacitor and V is the terminal voltage (V).

The main advantages of a supercapacitor are the long cycle of life being that it is capable of hundreds of thousands of complete cycles, high current capability due to the low value of equivalent series resistance (ESR). The ultracapacitor can deliver and absorb a very high current; simply monitored the state of charge (SOC), the energy stored is a function only of the capacitance and voltage, and the capacitance is constant. On the other hand, the main disadvantages are the low energy density and that it can be used for only a very short-term [16] [40].

2.3.2.2 Superconductor Magnetic Energy Storage

Although superconductivity was discovered in 1911, it was not until the 1970s that SMES was first proposed as an energy storage technology for power systems. SMES systems have attracted the attention of both electric utilities and the military due to their fast response and high efficiency (a charge/discharge efficiency of over 95%). Possible applications include load leveling, dynamic stability, transient stability, voltage stability, frequency regulation, transmission capability enhancement and power quality improvement [16].

An SMES unit is a device that stores energy in the magnetic field generated by the DC current flowing through a superconducting coil at cryogenic temperatures. This temperature is

maintained by a cryostat that contains helium or nitrogen liquid vessels. The inductively stored energy (*E* in joules) and the rated power (*P* in watts) are commonly given specifications for SMES devices. In general, when a current passes through a coil, the electrical energy will dissipate as heat due to the resistance of the wire. However, if the coil is made from superconducting material such as mercury or vanadium under its superconducting state, zero resistance occurs and the electrical energy can be stored with almost no losses. The system requires a considerable amount of energy to maintain the cryogenic condition and the current flow through non-superconducting material [16] [22]. Figure 12 shows the mechanism of SMES. Cooling of the superconducting coil is carried out using liquid helium at 4.2 Kelvin (K) (-296 °C) or liquid nitrogen at 77K (-196 °C), which is installed inside the adiabatic container (cryostat) [41].

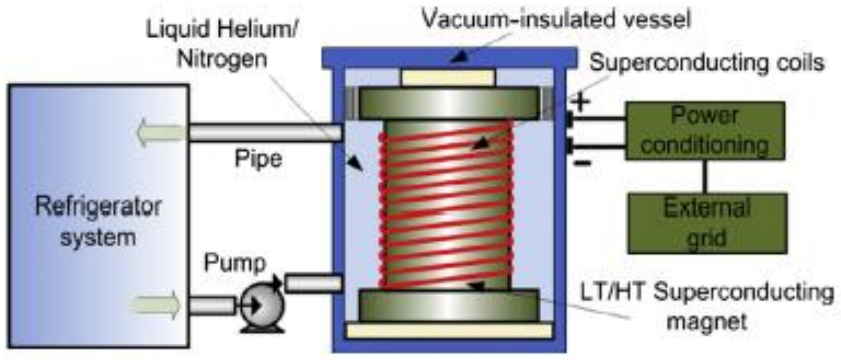

Figure 12 - Energy Storage using SMES technology.
Source: [36].

SMES topologies are cooled to a critical temperature depending on the type of superconductor. Superconducting coils can be classified into two groups [42]: low temperature superconductor (LT) coils, typically built with a Niobium-titanium (NbTi) alloy and cooled by liquid helium at about 4 K, and high temperature (HT) superconducting coils, generally made with a ceramic oxide compound in which the coolant is liquid nitrogen of about 70 K. The energy stored in the form of a magnetic field in the superconducting coil of a SMES is given by (4) [21].

$$E_{SMES} = \frac{1}{2} \cdot L \cdot I_L^2 \tag{4}$$

Where E_{SMES} is, the energy stored by the SMES system (J), L is the inductance (H) of the superconducting magnet and I_L is the inductor current.

Today's SMES systems are still expensive when compared with other energy storage technologies. However, the integration of an SMES coil into existing flexible ac transmission systems (FACTS) devices eliminates the cost of the inverter unit, which is typically the largest portion of the cost for the entire SMES system. Previous studies have shown that micro 0.1 MWh and midsize (0.1–100 MWh) SMES systems could potentially be more economical for power transmission and distribution applications [16].

2.3.3 Electrochemical Storage

Electrochemical energy storage technologies are one of the most widely used in industry and daily life. They consist of battery energy storage systems (BESS) that store electrical energy in the form of chemical energy. This storage methodology includes all traditional lead-acid battery, advanced battery, and redox flow batteries [36]. Generally, a battery contains two electrodes, one negative named the anode and one positive called cathode, an electrolyte which is either a liquid or solid that has the function of transporting the charges from the anode to the cathode. There exists a large number of battery technologies ranging from proven lead-acid batteries to more recent, but emerging ones, like lithium-ion batteries that all have different attributes and possible applications.

Some important parameters describe the present condition of the battery, those being [43] [44]:

- State of Charge (SOC) (%) – An expression of the present battery capacity as a percentage of maximum capacity. SOC is generally calculated using current integration to determine the change in battery capacity over time.

$$SOC = SOC(t_0) + \frac{1}{C_{rated}} \int_{t_0}^{t_0+\tau} (I_b - I_{loss})dt \tag{5}$$

  Where $SOC(t_0)$ is the initial SOC, C_{rated} is the rated capacity, I_b is the battery current, and I_{loss} is the current consumed by the loss reactions.

- Depth of Discharge (DOD) (%) – The percentage of battery capacity that has been discharged and is expressed as a percentage of maximum capacity. A discharge of at least 80 % DOD is referred to as a deep discharge.

Supposing that a battery is 100% fully charged, this means the DOD of this battery is 0%. Another example is if the battery has delivered 30% of its energy leaving 70% of the energy stored, then the DOD of this battery is 30%. Moreover, if a battery is 100% empty, the DOD of this battery is 100%. DOD can always be treated as how much energy the battery has delivered. For lithium batteries, we do not suggest fully discharging them to 100% DOD as it would shorten the life cycle of the batteries [43]. The relationship between SOC and DOD can be expressed by formula (6).

$$SOC = 100\% - DOD \tag{6}$$

An essential term is the battery's life cycle. Life cycle is a specification that attempts to define how many charge and discharge cycles a battery can experience before it fails to meet specific performance standards. A single cycle occurs when the battery is charged and then discharged. A key point to understand when interpreting a life cycle specification is that it is valid for a specific level of discharge. The higher the DOD, the lower the life cycle will be.

BESS technology has many valuable advantages. They are as follows:

- Rapid response time;
- Ready factory-built modules, which reduce construction lead time significantly.
- Best cost-benefit ratio between the other ESS technologies.

On the other hand, the main drawbacks of BESS technology include:

- The necessity for periodic maintenance;
- Limited life spans.
- Necessary temperature monitoring and control.

More details about some battery technologies will be given in the next section.

2.3.3.1 Lead-acid Batteries

The Lead-acid batteries are the oldest type of known rechargeable batteries. They were invented in 1859 by a French physicist named Gaston Planté. This particular battery is composed of several electrochemical cells connected in a series or parallel structure that produces electricity with the desired voltage from an electrochemical reaction. Each cell contains two electrodes (anode and cathode) with an electrolyte that can be in solid, liquid, or viscous states [36]. Figure 11 shows the basic structure of a battery. When connected to an

external load, the discharge of the battery occurs with the anode undergoing an oxidation reaction that releases electrons. The cathode attracts these negative ions and, consequently, the positive electrode has its material reduced. The discharge cycle is completed when the anions return to the anode and the cations to the cathode. The electric current has an opposite direction in charge of the battery. Thus in this way, the oxidation occurs in the positive electrode that becomes the anode and the reduction in the negative electrode which then becomes the cathode.

The advantages of lead-acid batteries include very short response times (in the range of milliseconds), low self-discharge rates (3% – 20% per month), relatively high cycle efficiencies (around 70%–85%) and low capital costs (100 – 200 U$/kWh). Other attributes are a favorable cost/performance ratio, easy recyclability and simple charging technology. However, the main disadvantages of lead batteries are the relatively low cycle lifetime (500–1200 cycles) and the low energy density of 50 – 110 Wh/L (specific energy around 30 – 50 Wh/kg). Other drawbacks of lead-acid batteries are the charging and discharging ability not being symmetrical, restrictions to the location of the installation and the necessity of ventilation [45] [46].

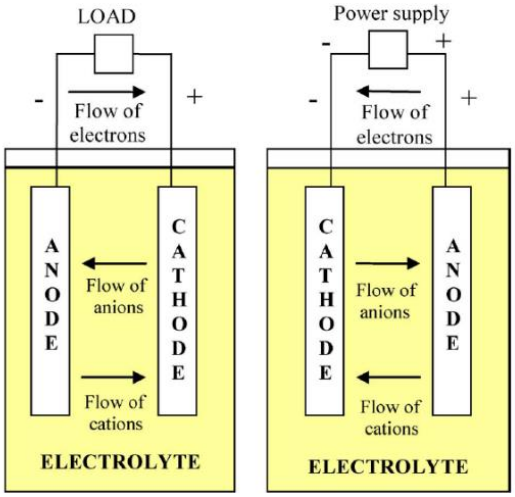

Figure 13 - Chargeable cell/battery diagram.
Source: [36].

2.3.3.2 Nickel-cadmium Batteries

Nickel-cadmium batteries use nickel hydroxide and metallic cadmium as the two electrodes and an aqueous alkali solution as the electrolyte. They typically have relatively high, robust reliabilities and low maintenance requirements. They have a specific power around 150 W/kg, a specific energy of 40–60 Wh/kg, a life cycle of about 2000 cycles, self-discharge rates of about 10% per month, cycle efficiencies around 70% – 90% and capital costs higher than

that of lead-acid batteries (around 300 – 600 U$/kWh). They also have relatively high reliability, safety (stable at deep discharges and overcharges) and low maintenance requirements. Furthermore, these are the only batteries with a good performance at low temperatures (−20 °C to −40 °C). Nevertheless, their major drawback is the use of cadmium and nickel, which are highly toxic heavy metals. Additionally, the appearance of a memory effect through which the maximum capacity of NiCd batteries can be dramatically decreased if the battery is repeatedly recharged after being only partially discharged.

2.3.3.3 Nickel-metal hydride Batteries

Nickel-metal hydride batteries have been introduced as battery technology in the 1990s to replace NiCd batteries. They are, in many aspects, superior to their Nickel cousin NiCd. They have approximately double the capacity of an equivalent size NiCd and an energy density comparable to that of a lithium-ion battery. NiMH batteries, with a nominal cell voltage of about 1.2 V, have a specific power of around 250 – 1000 W/kg, a specific energy of 60–120 Wh/kg, energy density of 140 – 400 Wh/L, cycle lifetime of 500 – 800 cycles (although newest commercial batteries reach 3000 cycles), cycle efficiencies of around 70% – 90% and less capital costs than NiCd batteries (around 200 – 500 U$/kWh).

Other advantages of NiMH batteries over NiCd batteries are that they suffer significantly less from the aforementioned memory effects and that they are more environmentally friendly (they can be more easily disposed of). Also, NiMH battery cells have lower internal resistance which makes them a preferred battery type for electronics with the high drain of current. However, the main disadvantage of NiMH batteries is the high rate of self-discharge (5–30%/month, highly time-dependent). They are also less robust than NiCd batteries, have a low tolerance against overcharging and are more sensitive to deep cycling (their performance decreases after a few hundred full cycles). Thus, NiMH batteries are generally used for portable products, mobile applications in (hybrid) electric vehicles and potential industrial standby applications, such as uninterruptible power supply (UPS) devices.

2.3.3.4 Lithium-ion Batteries

Lithium-ion (Li-Ion) batteries have been commercially available since 1990. The electrolyte is usually a non-aqueous organic liquid containing lithium salts, such as LiClO4 or LiPF6, that is dissolved in organic carbonates. When the battery is charged, the lithium atoms in the anode become ions and migrate through the electrolyte toward the cathode where they combine with external electrons and are deposited between carbon layers as lithium atoms. Discharging reverses this process.

Foremost advantages of Li-Ion batteries technology are a high-energy density (250–600 Wh/L, better than those of NiMH batteries), high specific energy (75–265 Wh/kg), short response time (ms), a long life cycle (400–1500 cycles, although newest commercial batteries exceed 3500 cycles), a low self-discharge (around 2%–5% per month), a specific power around 250–2000 W/kg and very high cycle efficiencies around 90%–97%. Other benefits of Li-Ion batteries over NiMH ones are that they do not suffer from the memory effect, high performance, long lifetime, and they are more environmentally friendly.

The capital costs of Li-Ion batteries are slightly higher than those of NiCd batteries (around 300–700 U$/kWh), but the expansion of global production capacity is continuously bringing down these costs. The market for batteries of electric and hybrid vehicles is growing slowly but steadily. Thus, the latest lithium-ion batteries costs have collapsed particularly over the last five years during which costs have fallen to below 300 U$/kWh today.

Lithium-ion batteries are mainly used as medium-term energy storage but can also be used as short-term storage. They have become an essential storage technology in portable applications (*e.g.*, laptop, cell phone) during recent years. Also, in electric vehicles, mainly lithium-ion batteries are used. In stationary applications, they can be an attractive option as well. Several demonstration projects with lithium-ion battery containers exist in Europe whereas in the US, lithium-ion battery storage containers are already used in weak grid areas.

2.3.3.5 Sodium-sulfur Batteries

Sodium-sulfur (NaS) battery systems have been in commercial use since the mid-1990s. They are a type of molten-salt battery built from liquid sulfur (molten Na) at the positive electrode and liquid sodium (molten S) at the negative electrode separated by solid beta alumina (beta- Al2O3) ceramic tube, which acts as both the electrolyte and separator simultaneously

[36]. A Na-S battery assembly consists of three major subsystems: a large number of electrically and mechanically interconnected cells, a thermal enclosure maintaining a temperature in the range 300–350 °C, and a heat management system for initially heating and removing waste heat from battery [47].

The conventional Na-S battery is required in order to operate at a temperature of about 300 °C to keep the electrodes (sodium and sulfur), as well as the reaction product polysulfide in a liquid (molten) state (although NaS BESSs are presently being developed with lesser temperatures as low as 100° C). This feature supports the high reactivity of electrodes. As a result, significant benefits of NaS batteries are high-power and energy densities (specific power 150–300 W/kg and specific energy 150–240 Wh/kg), high efficiency (roundtrip efficiency about 80%–90%), long lifetime (around 2500 cycles), fast response (ms) and high pulse power capability. Furthermore, they have excellent temperature stability and safety levels, with capital costs of around 250–500 U$/kWh.

They are demonstrated to be suitable as grid energy storage for non-mobile, large-scale applications with daily cycling, such as peak shaving, load leveling, emergency power supply, and as a support for the integration of renewable energy generation. Nonetheless, the main drawback of NaS battery systems is the requirement of a heat source to maintain operating temperatures which uses the battery's own stored energy, partially reducing the battery performance.

2.3.3.6 Flow Batteries

A flow battery energy storage (FBES) is a form of battery in which the electrolyte contains one or more dissolved electroactive species flowing through a power cell/reactor in which the chemical energy is converted into electricity. An additional electrolyte is stored externally, generally in tanks, and is usually pumped through the cell (or cells) of the reactor. The reaction is reversible, allowing the battery to be charged, discharged, and recharged. In contrast to conventional batteries, flow batteries store energy in the electrolyte solutions.

The power and energy ratings are independent of the storage capacity determined by the quantity of electrolyte used and by the power rating of the active area of the cell stack. Flow batteries can release energy continuously at a high rate of discharge for up to 10 hours. Flow batteries are also distinguished from fuel cells by the fact that the chemical reaction involved is

often reversible, *i.e.*, they are generally of the secondary battery type and thus can be recharged without replacing the electroactive material [27].

The most significant feature of flow batteries is the independence between their power and energy ratings, which brings a flexible layout. Other advantages include a long life cycle (3000–5000 cycles), round-trip efficiency of 70%–85%, very robust, short response time (ms), low, self-discharge (1% per day), tolerance to overcharge/over-discharge, no need for equalization during charging, low maintenance, and no harmful emissions. The capital costs of redox flow batteries are around 200-300 U$/kWh [46].

A major advantage of flow batteries is that the power of an FBES system is independent of its storage capacity. The power of an FBES system is determined by the size of the electrodes and the number of cells in the stack, whereas the storage capacity is determined by the concentration and the amount of electrolyte. Also, an FBES can provide a fast response to the grid demands, minimum maintenance and zero CO_2 emissions. Drawbacks of flow batteries include relatively high manufacturing costs, more complicated system requirements compared to traditional batteries, and compared to other batteries technologies, the power density and energy is very low [48].

The most important commercially available type of flow battery is the Vanadium Redox-Flow Battery. This battery type is, for example, available from Cellstrom (Austria) and Prudent Energy (USA) with different modular, scalable sizes. Several demonstration sites with this technology exist, particularly in Japan where it is used mainly for load-leveling purposes in the range of several 100 kW. Zinc-Bromine batteries are another type of flow battery which are also commercially available [26].

2.3.4 Chemical Storage

Chemical energy is the type of energy that is stored in molecular compounds. In particular, it is stored in the bonds between different types of molecules. When something causes these bonds to break, the molecules rearrange themselves and the energy is released. The substance from which the energy came is changed into an entirely different element and often into another energy form [26]. Chemical energy storage mainly focuses on secondary energy carriers such as hydrogen and synthetic gas (a mixture of hydrogen and carbon monoxide) [65].

2.3.4.1 Hydrogen Energy Storage

Hydrogen energy storage (HES) is one of the most widespread types of chemical energy storage. Hydrogen is the lightest and simplest in addition to being one of the most abundant elements found in nature. It can always be found as arranged with other elements and has a variety of useful properties. In addition, it is considered the fuel that has the highest energy per mass when compared to the other fuels. However, its lower density at ambient temperatures requires the development of advanced storage technologies in order to reach higher energy density. Figure 14 shows the topology of hydrogen storage and fuel cells. There are several ways to store hydrogen, such as in gaseous or liquid form. The storage of hydrogen gas in metal tanks is currently the cheapest, most mature and most reliable method known. In this way, hydrogen can be stored for several hours (up to 30 h) without noticeable losses [49].

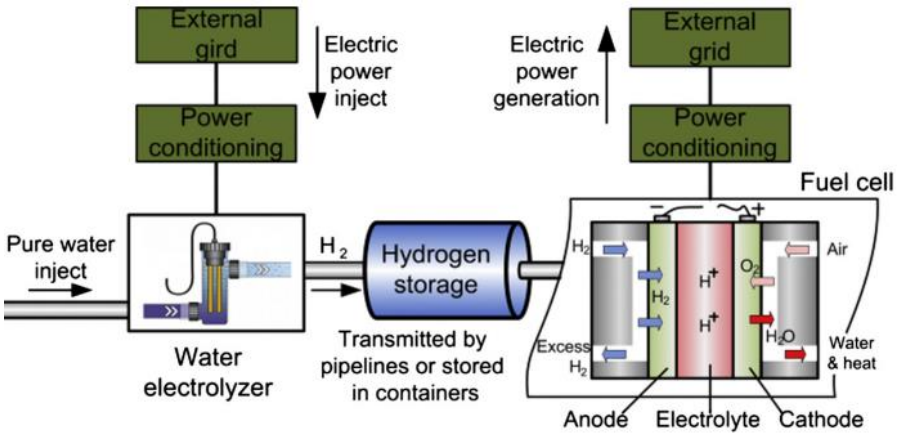

Figure 14 - Topology of hydrogen storage and fuel cells.
Source: [36].

Hydrogen-based chemical energy storage systems use two separate processes for storing and releasing energy. To generate electricity, the electrolyzer converts the water into hydrogen and oxygen gas. Both gases (hydrogen and oxygen) are fed into a fuel cell in which an electrochemical reaction (an oxidation half-reaction occurring at the anode and a reduction half-reaction occurring at the cathode) takes place. The anode and the cathode are separated from each other by the membrane that acts as an electrolyte.

Hydrogen and oxygen react and generate electricity while producing water and releasing heat. The use of an electrolyzer is a common way to produce hydrogen from water which can be stored in high-pressure tanks for later use. This can be done practically for an unlimited amount of time. In this sense, regenerative fuel cells are devices that combine the

function of the fuel cell and the electrolyzer into one single device [50]. Combining the two features into one device reduces the system size. Nevertheless, current regenerative full cell designs are less efficient in hydrogen production than other methods such as combined electrolysis-fuel cells.

In general, the electricity generation by using fuel cells is quieter, produces less pollution and is more efficient than the fossil fuel combustion approach. Other features include easy scaling (potential from 1 kW to hundreds of MW) and compact design.

2.3.5 Thermal Storage

Thermal Energy Storage (TES) already exists in a broad spectrum of applications. It includes a variety of technologies that store heat by using different ones in the insulated repository. It uses materials that can be kept at high and low temperatures in insulated containments.

Thermal energy storage can be categorized into three technologies depending on what they use. The sensible heat storage is a method involving a temperature change of a material (sodium, molten salt, pressurized water, concrete, *etc*.), latent heat storage through a phase change of a material (liquid-solid transition at constant temperature) and thermochemical heat storage by thermally inducing changes in a material chemical structure (using an adsorbent/working fluid pair). Nonetheless, in the context of electrical energy storage, sensitive/latent heat storage systems are the most relevant and cryogenic energy storage (CES) under development [51] [27]. The choice of the TES technique depends on multiple issues such as the storage temperature range, the specific application and the storage media.

2.3.5.1 Sensitive Heat Storage

Sensitive heat thermal storage is the most straightforward technology that exists. It is based on heating or cooling a liquid or solid storage medium and is one of the best known and most extensive technologies that exists. This medium does not undergo any form of phase change. The storage medium can be a liquid such as water or thermal oil, or a solid such as concrete or the ground. The specific heat capacity and the mass of the medium used are applied in order to define the capacity of a storage system. Sensitive heat storage is not only cost

efficient and environmentally friendly, but it can also be easily stored as bulk material, enabling a simpler system design.

2.3.5.2 Latent Heat Storage

Latent heat storage is accomplished by using phase change materials (PCMs) such as organic (paraffin) and inorganic materials (salt hydrates) as a storage medium. Latent heat is the energy exchanged during a phase change. It is also called “hidden heat” because there is no change of temperature during the energy transfer. Currently, most PCMs use the solid-liquid phase change like molten salts as a thermal storage medium. Latent heat storage can be smaller, more efficient, and can provide a lower cost alternative to sensitive thermal storage systems. The available storage capacity of PCM is 100 kWh/m³ as opposed to 25 kWh/ m³ for sensitive heat storage systems [52].

TES systems can store large quantities of energy without any significant hazards. The heat cycle efficiency (70%–90%) and its daily self-discharge losses are small (around 0.05%–1%). Furthermore, the reservoir offers good energy density and specific energy. However, the overall round-trip cycle efficiency of a TES system is low (30%–45%). Moreover, TES is technically developed and commercially available, but their actual applications, especially for large-scale utility, are still not widespread. It has been used in applications such as load shifting and electricity generation for heat engine cycles [27] [53].

2.3.5.3 Cryogenic Energy Storage

Cryogenic Energy Storage (CES) is a new electrical energy storage system that is identified as a class of thermal energy storage [54]. Off-peak power generates cryogen (*e.g.*, liquid nitrogen or liquid air) or renewable generated electricity through direct mechanical work from a hydro or wind turbine (in which electricity is stored). During the peak time, heat from the surrounding environment boils the liquid and the heated cryogen is used to generate electricity using a cryogenic heat engine (electricity is released). At the same time, the waste heat from the flue gas of the power plant, if and when available, can be used by the CES. Cryogenic Energy Storage (CES) is sometimes referred to as Liquid Air Energy Storage (LAES).

The LAES cycle consists of three main elements: a charging system, a discharge system and a storage system. The principle of such a technology is shown in Figure 15. While charging, ambient air is first compressed, cooled and then expanded to produce liquid air. The liquid air is then stored at low pressure in an insulated storage tank. During discharge, the liquid is drawn from the tank, compressed, heated and expanded in order to produce work that can in turn be used to generate electricity. The cycle efficiency can be improved significantly by recovering and storing the cold thermal energy released during the heating of the cryogenic fluid during discharge, and by using this to pre-cool the high-pressure air before expansion cooling during charging. This 'cold recycle' thermally couples the charging and discharging processes by way of a (cold) thermal store [54].

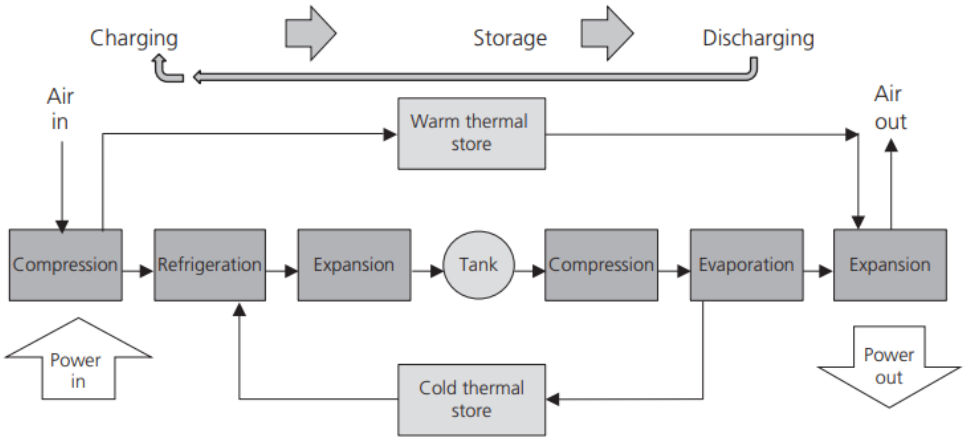

Figure 15 - Schematic diagram of CES.
Source: [54].

CES can also provide direct cooling and refrigeration, air conditioning units as well as act as a power source for vehicles. CES can have a relatively high energy density (100 – 200 Wh/ kg). The low capital cost per unit energy can be benign to the environment and can have a relatively long storage period. However, CES has a relatively low efficiency (40 ~ 50%) according to the current energy consumption for air liquefaction. CES is still under development by the University of North Texas (USA) and the University of Washington (USA) Mitsubishi (Japan), the University of Leeds (UK) and the Chinese Academy of Sciences (China) [27].

CES systems use off-the-shelf components with long life (30+ years) resulting in low technology risk, can be built anywhere and have zero emissions and good materials along with more than 70% of efficiency by using waste heat or cold.

Table 3 summarizes the state of most energy storage technologies [55].

Table 1 – Energy Storage Technologies.

Technology	Primary Application	Benefits	Challenges
CAES	•Load leveling; •Frequency regulation; •Peaking shaving and of peak storage; •Transient stability.	•Modular technology; •Long life cycle; •High peak power without overheating concerns; •Rapid response; •High round trip energy efficiency.	•Rotor tensile strength limitations; •Limited energy storage time due to high frictional losses.
PHS	•Energy management; •Backup and seasonal reserves; •Regulation service.	•Developed and mature technology; •Very high ramp rate. •Currently most cost-effective form of storage.	•Geographically limited. •Plant site; •Environmental impacts; •High overall project cost.
FES	•Load leveling; •Frequency regulation; •Peak shaving and off-peak storage; •Transient stability.	•Modular technology; •Proven growth potential to utility scale; •Long cycle life; •High peak power without overheating concerns; •Rapid response; •High round trip energy efficiency.	•Rotor tensile strength limitation; •Limited energy storage time due to high frictional losses.
Lead-Acid Batteries	•Load leveling and regulation; •Grid stabilization.	•Mature battery technology; •Low cost; •High recycled content; •Good scaling potential.	•Limited depth of discharge; •Low energy density; •Large footprint; •Electrode corrosion limits useful life.
NaS	•Power quality; •Congestion relief; •Renewable source integration.	•High energy density; •Long discharge cycles; •Fast response; •Long life; •Good scaling potential.	•Operating temperature required between 250°C and 300°C; •Liquid containment issues (corrosion and brittle glass seals).
Li-ion	•Power quality; •Frequency regulation.	•High energy densities; •Good cycle life; •High charge/discharge efficiency.	•High production cost scalability; •Extremely sensitive to over temperature, overcharge and internal pressure buildup; •Intolerance too deep discharge.
Flow Batteries	•Ramping; •Peak shaving; •Time shifting; •Frequency regulation; •Power quality	•Ability to perform high number of discharge cycles; •Lower charge/discharge efficiencies; •Very long life.	•Developing technology, not mature for commercial scale; •Complicated design; •Lower energy density.
SMES	•Power quality; •Frequency regulation.	•Highest round-trip efficiency from discharge.	•Low energy density; •Material and manufacturing cost prohibitive.
Supercapacitors	•Power quality; •Frequency regulation.	•Very long life; •Highly reversible and fast discharge.	•Currently cost prohibitive.
TES	•Load leveling and regulation; •Grid stabilization.	•Extremely high energy densities.	•Currently cost prohibitive.

2.3.6 Challenges and prospects

It is no doubt that energy storage can help to reduce energy wastage and greenhouse gas emissions as well as increase the penetration of renewable energy resources. As presented in the previous chapters of this thesis, several energy storage technologies have been developed throughout the past decades. Some of these ESS have been successful. For example, PHS and CAES technology have been used for decades with proven reliability and availability. Advancement in battery technology has resulted in more robust and efficient battery technologies with high power and energy density. Despite all of these advancements:

- One of the main challenges (especially of large-scale energy storage technologies such as PHES and CAES) is how to improve the roundtrip efficiency. An ideal energy storage technology is one which can achieve a roundtrip efficiency of 100%. Although this is not possible in real life application, an energy storage technology should aspire to achieve round trip efficiency as close as possible to 100% in order to reduce the gap between their potential and operational success. Theoretical prediction for PHES shows that they can potentially attain an efficiency of 90%. However, most of the real-life installations have shown a roundtrip efficiency of 72–75%. In the same vein, CAES shows efficiency of about 42–55%. The challenge lies in identifying how to improve these efficiencies [56].
- Another challenge is that of system economics. The economics of energy storage is difficult to evaluate since it is influenced by a wide range of factors including: the type of storage technology, the requirement of each application and the size and system in which the storage facility is located. Most of the energy storage technologies are still very expensive whereas the incentive lies in making these technologies cheap. The reason for this is that energy storage technologies are usually used to store electricity which is a relatively cheap commodity, and thus for these technologies to be economically viable and attractive to investors, it needs to be cheap as well. Figure 16 (a) and (b) shows the capital costs of different energy storage technologies per unit of power ($/kW) and per unit of energy capacity ($/kWh).

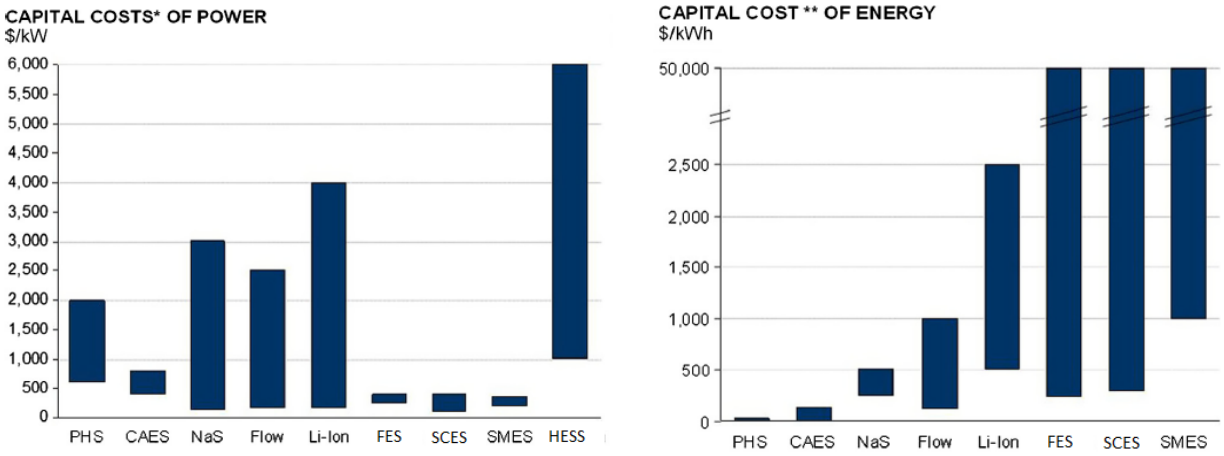

Figure 16 - (a) Capital cost of energy storage per unit power and (b) per unit energy capacity. Source: [56].

- The third challenge faced by this sector is the unavailability of standard for the physical connections of different energy storage solutions in the electricity grid. There is still too much complexity in the entire design of some energy storage technologies, which makes it challenging to develop modular energy storage systems. Although some energy storage technologies such as batteries are already standardized and modularized, most of the other energy storage technologies have still not accomplished this feat. Modularization of the energy storage technologies helps to promote the flexibility that the system provides. It allows for more optimization of the system behavior in response to changing conditions.
- In addition to these challenges, in order for energy storage to prosper, there is also a need for policy support from the government. This will enhance the penetration of energy storage, especially for grid application. For example, the UK electricity grid is expected to reach 110 GW by 2020 and the government aims to generate 30% of this energy from renewable sources. The government is currently funding energy storage research to achieve this aim.

Having discussed these challenges and barriers, it is understood that in a general way, the main solutions consist of establishing appropriate markets, technologies, policies and incentives. Also, it is necessary to finance R&D programs in the area to stimulate the development of technologies. In conclusion, the incentive to the commercialization is also very important since the increase of the production would contribute to the fall in the price of alternative ESS. However, an effort by governments, industry, universities, research centers and investors is additionally necessary.

CHAPTER 3 - FLOW REGULATION REVIEW

The sizing of the storage capacity of a reservoir is not a new problem in water resource management. The unconstrained form of this problem poses the question: “how large must the storage capacity of a reservoir be to provide a steady supply of water of a demanded magnitude?” A constraint that must be made for the problem is that the supply and demand cannot be higher than the mean discharge of the stream as it is impossible for a reservoir of any size to supply more water than it receives over an extended period. Another constraint that has to be made is that a reservoir may not be able to guarantee an uninterrupted provision even if the demand is smaller than the mean inflow discharge due to stochastic nature of the streamflow process. On account of the fact that there is no future inflow record, the traditional approach to this problem has been to determine the storage capacity of the reservoir by the past streamflow record and assume that the future will not be different from that of the past [57] [58].

According to McMahon et.al. (1978), the capacity required for the storage depends on three main factors: the variability of the river flows, the demand and the reliability of this demand being met [59].

Some graphical methods were developed to determine the storage capacity of a reservoir. This method was introduced by Rippl (1883) and marked the beginning of rigorous reservoir theory. Despite this, a few ideas about the flow regularization techniques applied in the reservoir are discussed below.

3.1 Rippl Diagram

According to Vilella et al. (1979), the mass diagram is defined as the hydrographs integral [60]. In 1883, Rippl introduced this technique to analyze the water reservoir. Conforming to Klemes (1979), Rippl’s original method proposed two significant modifications: the diagram would be plotted with the residual mass curve, and the replacement of the critical period would fill up [61]. The evolution of the mass curve technique is shown in Figure 17.

The Rippl diagram or mass diagram can be defined by how the stored volume of water in a reservoir flows in a given period of time. This technique is used to determine the cumulative flow departures with respect to the draft as well as for draft determination or the flood reduction

corresponding to given storage, optimum flow-equalization, the hydro-plant operation for given power output, reservoir rule-curves, etc.

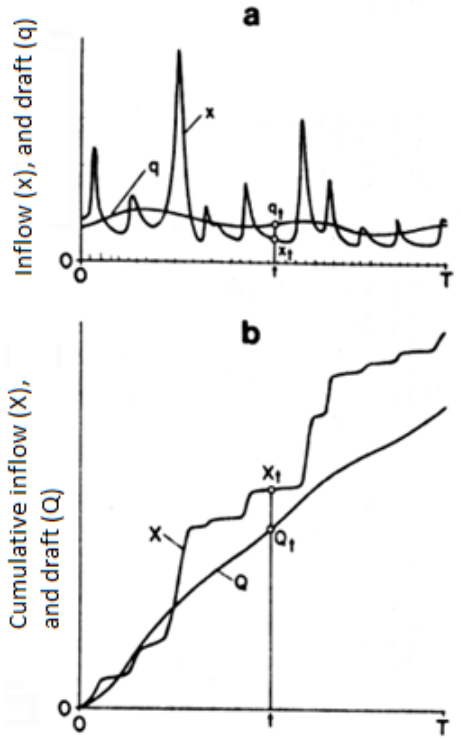

Figure 17 - Evolution of mass diagram for Rippl's method.
Source: [61].

Where:

(a) Represents the inflows hydrographs;

(b) Mass curves of inflow X and draft Q;

In differential terms, the accumulated volume in function of the time is shown in (7).

$$dV = Q.dt \tag{7}$$

In other words, this expression can be compared to the area under the curve in which volume is equal to the sum of elapsed flows (8).

$$V = \int_{ti}^{tf} Q.dt \tag{8}$$

In Figure 18, the diagram for a rain profile is shown. It can be seen that the curve is composed of line segments (B and C). These points are greater or less than the inflows, depleting the reservoir in the period. Thus, points B and C are critical periods and can be used

to define the reservoir capacity. Any type of flows can obtain these segments: hourly average, daily, weekly, monthly, annually, or instantaneously. Mathematically, it can be obtained by (6). Points B and C are the respective maximum and minimum volume values in comparison to a given yield. The slope describes the average flow ($\bar{Q}$) of a period proportional to the change in volume divided by the length of the period (9).

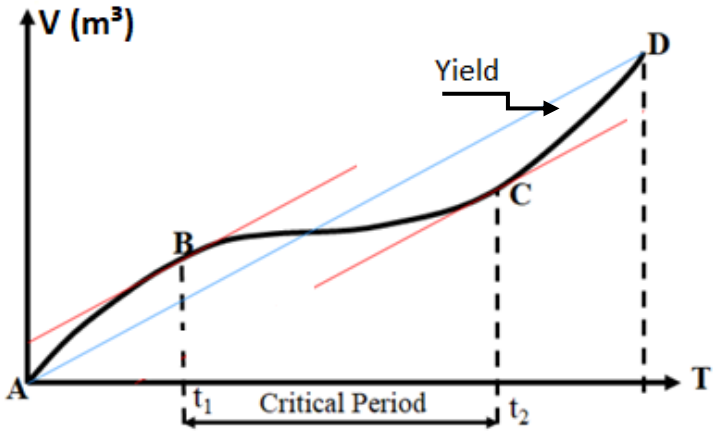

Figure 18 - Rippl diagram and cumulative volumes.

$$\bar{Q} = \frac{\Delta V}{\Delta T} \tag{9}$$

The Rippl diagram, in addition to its other possibilities, allows for the determining of the critical period, the average flow rate in the period and the study of flows regularization.

3.2 Differential Rippl Diagram

Another way to analyze the flow rates indicated in rain profile is by calculating the Differential Rippl diagram or accumulated volume (V_D) [62]. This diagram is used to find the smallest storage capacity necessary to supply the desired draft without failure throughout the period (T) and also allows for assessing the flows in relation to $\bar{Q}$ of the period, which is nothing more than a change of reference on Rippl's diagram. Mathematically, this method can be described as an integral or sum between the difference of instantaneous flow $Q(t)$ and the average flow ($\bar{Q}$), as defined by (10) [8].

$$V_D(t) = \sum_{t=1}^{j} [Q(t) - \bar{Q}\,] \tag{10}$$

The capacity of the reservoir (V_U) is calculated by using the difference between the maximum and minimum value of the Differential Rippl diagram that would attend in the most critical periods of dry season with an average flow, and in our case, the period of sun absence. Figure 19 shows the Differential Rippl diagram and the maximum and minimum values necessary to calculate the volume for total regularization.

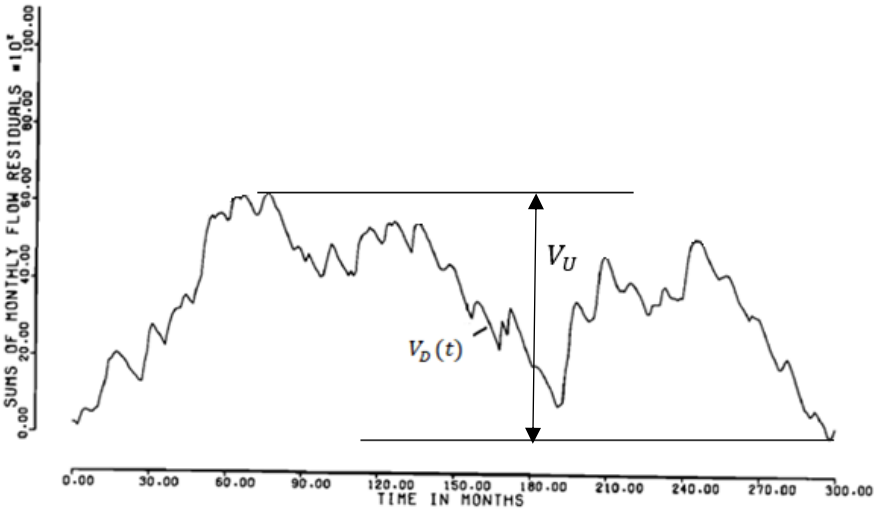

Figure 19 - Differential Rippl diagram.

3.3 Conti-Varlet Technique

In 1923, Varlet developed a method called the “stretched-thread rule.” According to Klemes (1979), the use of the stretched-thread method to find the inflow regularization of the reservoir is quite satisfactory with a maximum accuracy possible since no discretization is employed [61].

The Conti-Varlet is a technique that is evolved from the Rippl diagram. The Rippl diagram is used in total flow regularization while the Conti-Varlet is used in partial flow regularization. However, the primary objective is the same: keep the flow constant in maximum value in time without undesirable spills [12]. In statistical terms, the Conti-Varlet represents the minimization of the standard deviation of the regularized flow. While the Rippl diagram

indicates a flow, which is the mean to be guaranteed throughout time, the Conti-Varlet diagram shows a series of flow rates which are “greater and more constant” in their intervals.

Linear programming and dynamic programming are also used. However, these techniques have limited accuracy depending on the coarseness of the discrete representation of the storage and draft ranges. The time required for the dynamic programming solution grows with an increase in reservoir storage capacity. It decreases in the case of the stretched method, thus defying the ‘curse of dimensionality.’ The dynamic programming on account of the number of state variables and linear programming because of the number of equations to be solved.

The Conti-Varlet is the differential Rippl diagram added by a given volume. This volume, in hydropower plants, is the utile volume indicated by two limit quotes, the upper and inferior reservoir quotes, as shown in Figure 20. For each period, the dislocated Differential Rippl line $V_{DR}(t)$ is obtained:

$$V_{DR}(t) = V_D(t) + V_u \tag{11}$$

Where $V_D(t)$ is the Differential Rippl diagram and V_u is the utile volume for the reservoir.

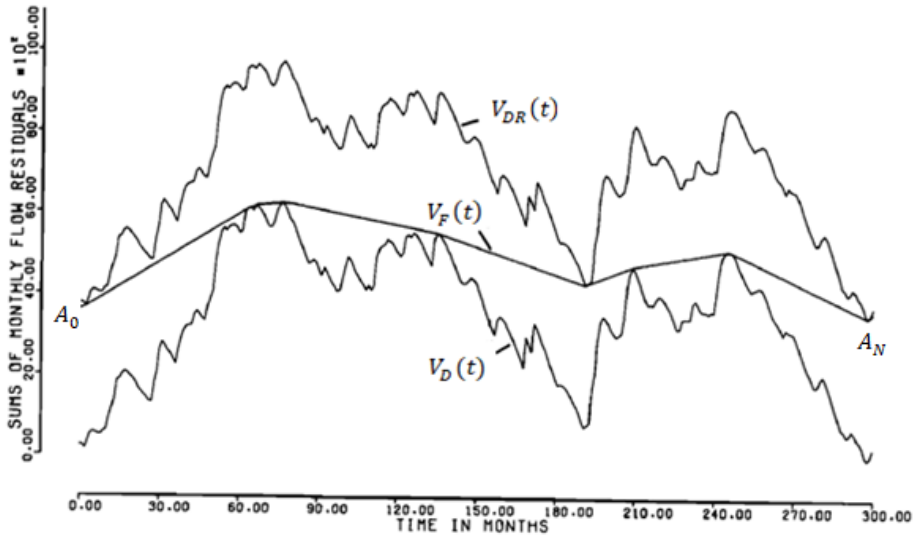

Figure 20 - Conti-Varlet Diagram.

The $V_F(t)$ is the optimal reservoir outflow obtained by the stretched-thread method and represented by the shortest path between two points A_0 and A_N at the opposite ends of a corridor formed by two mass curves described above.

Mathematically, the volume $V_F(t)$ is obtained through the Stretched-Thread method that is similar to the Shortest Path technique where the upper and lower limits in each period of time are given by $V_{DR}(t)$ and $V_R(t)$ respectivelly. Thereby, the flow regularized in each period is given for the following expression (12):

$$Q_F = \overline{Q} + \frac{dV_F}{dt} \tag{12}$$

The STM described here is based on [61]. This method is used when the corridor is enclosed within two broken lines consisting of straight-line segments and when the endpoints of the shortest path are specified. The lower broken line is given by V_D and the broken upper line as V_{DR}. To draw the V_F curve, a procedure is described below:

1. A straight line connecting the endpoints A_0 and A_N is computed;
2. The corridor boundaries are checked to see whether any of them are crossed by line $A_0\ A_N$. If no crossing is recorded, line A_0A_N is the desired shortest path. If V_D crosses A_0A_N, the point of maximum distance of V_D above A_0A_N is identified as a corner point A_i of the shortest path; if V_{DR} crosses A_0A_N, then the point of maximum distance of V_{DR} is identified as another corner point A_j;
3. The corner point closest to the starting point A_0 is regarded as an end point of the shortest path in the period (0, j).
4. Steps 1-3 are repeated with A_j replacing A_N;
5. If no additional corner points are identified in the interval (0, j), the straight line A_0A_j is the first segment of the shortest path and the search moves to the next interval (j, i) with A_j and A_i representing the starting and end points, respectively. If, however, an additional corner point A_k, is identified in the period (0, j), the search moves to the interval (0, k).
6. In general, the search always moves forward in time only after the shortest path in the whole past period has been found.

In statistical terms, when more storage is available in the system, more flow becomes regularized. In this way, the standard deviation will decrease by the same proportion. In other words, the reservoir would have to pursue a defluent flow, which approaches the average flow by defining an operation policy in order to minimize the mean-square deviation over time, as in accordance to (13). Also, this proves that the Conti-varlet diagram provides a constant flow in all periods that are higher or more constant in their intervals.

$$min_z = \sum_{i=1}^{T} (\overline{Q} - Q(t))^2 \tag{13}$$

These methods aforementioned can also be applied in renewables sources such as wind and sun since they share similar physical phenomena characteristics. The use of these techniques provides an estimate of the sizing of a storage system that reduces the impact of these uncertainties providing a constant power in the period chosen for the regularization and reducing the mismatch between generation and load demand. Table 2 shows the similarities found between the formulas used in the flow regularization and, in our case, for power regularization.

Table 2 - Formulas comparison.

Flow	**Power**
$dV = Q.dt$	$dE = P.dt$
$V(t) = \int_{t_1}^{t_2} Q.dt$	$E(t) = \int_{t_1}^{t_2} P.dt$
$Q_F = \overline{Q} + \frac{dV_F}{dt}$	$P_F = \overline{P} + \frac{dE_F}{dt}$

CHAPTER 4 - OPTIMIZATION METHODS TO SIZE BESS

The concept of optimization refers to decision-making that improves a particular process by starting from a mathematical formulation of the problem. The first challenge in the optimization process is the definition of a mathematical model that represents the real problem. In other words, this formula needs to reflect all of the premises and difficulties inherent to the real problem that is desired to be optimized. The objective function, which must be coherently related to the variables of the problem, is responsible for representing a quality measure for each of the solutions generated by the optimization algorithm, so the best solution to the problem is represented by a composite vector by the values of the design variables that optimize the objective function. The constraints, which need to be related to the variables of the problem, have the objective of avoiding the optimization algorithm considered as the best result solutions that, in practice, are considered unfeasible [63].

A usual way to represent a given problem mathematically is to write it as follows:

Optimize:

$$F_{obj}(X) \tag{14}$$

The constraints are:

$$a_{min} \leq X_i \leq a_{max} \text{ ; for i=1,…,n} \tag{15}$$

$$G_j(X) \geq 0 \quad \text{; for j=1,…,p}$$

$$H_k(X) = 0 \quad \text{; for k=1,…,m}$$

Where optimizing refers to maximizing or minimizing, being X =[X_1, X_2,…, X_n] a vector of n dimensions that represents the variable of the project. Each variable X_i, has a limit inferior a_{min} and a limit superior a_{max}. The $F_{obj}(X)$ is the objective function that is related to the system variable performance of vector X, $G_j(X)$ which is the *j-th* inequality constraint and where $H_k(X)$ is the *k-th* equal constraint applied on X.

When considering the storage system in a grid, an optimal storage system sizing should be performed. The small storage systems may not provide economic benefits and desired

flexibility in power generation of other units for the grid as much as expected. On the other hand, large storage systems impose higher investment and maintenance costs to the network. Therefore, an optimal size for the storage system should be found where the produced reduction in operating cost due to the addition of the storage system is larger than the installation costs imposed by storage. Figure 21 depicts the optimal size of a storage system regarding investment, maintenance, and operating costs.

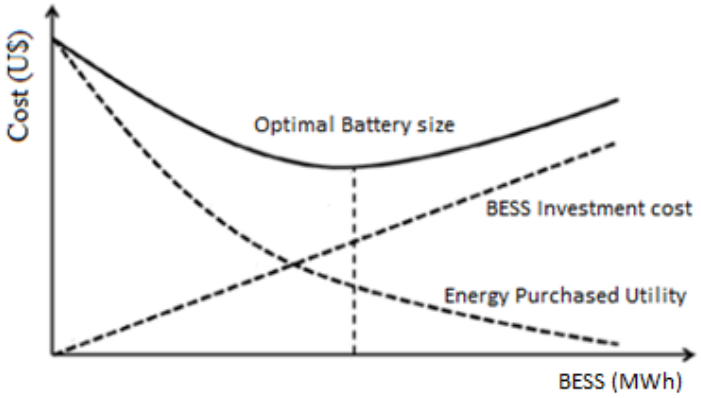

Figure 21 - Grid expansion planning cost vs. BESS size.

As the BESS is increased, the investment cost is added to the battery in a linear fashion while the cost of the energy provided by the utility is reduced. The minimum value of the average cost curve can be seen as the optimal size for a given BESS since this point would minimize the total cost of energy consumed by the community. In other words, this would be the cost for changing consumption (disutility) [64].

4.1 Methods of BESS Sizing

Nowadays, the energy storage system sizing for power and energy application has been widely investigated in *academia*. Studies on sizing BESS can be determined using a wide variety of techniques for both on-grid and off-grid applications [65]. For example, the IEEE 1013 standard provides sizing recommendations for lead-acid batteries in stand-alone PV systems [66]. The BESS sizing difficulty varies since a probabilistic technique goes through to mathematical optimization. In this chapter, the following methods are discussed: probabilistic, analytical and direct search-based.

4.1.1 Probabilistic Methods

Probabilistic methods are perhaps the most intuitively appealing and straightforward approaches in battery sizing. The key concept is to use the stochastic nature of the renewable resources, typically solar or wind, in order to optimize the battery size for the selected criteria. The probabilistic method is commonly used in situations when occurring data is absent. A drawback of this is the number of performance criteria being optimized in these approaches tends to be small, which makes their applicability for detailed systems limited.

One approach is the use of statistical methods to generate simulated samples. The Global Horizontal Irradiance (GHI) data of solar irradiance have been generated through a Markov-chain approach for BESS sizing [67]. Besides implementing probabilistic methods for data generation, stochastic optimization methods have also been deployed in many studies. The most popular technique in these approaches is the Monte Carlo technique in which a large number of scenarios are generated according to the statistical behavior of random variables. The Monte Carlo approach requires a significant computational effort. However, it also offers a comprehensive strategy for making a design decision.

Authors in Wu et al. (2014), presented a mixed distribution based on Laplace and normal distribution to model forecast errors associated with persistence forecast for a single wind farm over multiple timescales. Thus, the proposed distribution is used to estimate the penalties for prediction errors in the electricity market. A probabilistic method is proposed to determine the optimal size of ESS for a wind farm in electricity markets. It is shown that through minimizing the penalty cost from forecast errors, along with the cost of the ESS, the optimal energy and power capacity of ESS can be obtained. The results demonstrate that the proposed distribution and probabilistic method is efficient enough to find an optimal size of ESS [68].

The authors Yu et al. (2015), used a probabilistic approach to properly size the BESS from the perspective of the inertial system response as an application of probabilistic risk assessment. The proposed method enables a risk-informed decision-making process regarding the acceptable level of solar penetration in a given system and the desired BESS capacity (and minimum cost) to achieve an adequate grid inertial response with a certain confidence level. The results showed that the approach used can be used to size the ESS that mitigates frequency impacts on the grid in cases of reduced grid inertia and large power mismatches introduced by undispatchable renewable resources [69].

A novel method is proposed by the authors Bludszuweit (2011), for design an ESS that is dedicated to the reduction of the uncertainty of short-term wind power forecasts up to 48

hours. The investigation focuses on the statistical behavior of the forecast error and the state of charge (SOC) of the ESS. This approach gives an insight into the influence of the forecast conditions (horizon, quality) on the distribution of SOC. A one-year time series of power output measurements and forecasts are available for two-wind farms. The proposed probabilistic method permits the sizing of energy storage systems as a function of the desired remaining forecast uncertainty, reducing power and energy capacity simultaneously [70].

Ovelha (2017) proposed a design and the sizing of an off-grid PV system with a battery energy storage system for a residence located in Portugal. The load demand is considered in order to size the system. With the system's components calculated, a software called HOMER is used to understand the sized system. Also, an economic analysis is provided showing that the system is not economically profitable since its Net Present Value is negative for a scenario when the energy is entirely supplied by the PV and battery system. In the second case, the PV system is connected to the grid and the Net Present Value shows a positive value along with the payback time of investment which is almost 12 years [71].

4.1.2 Analytical Methods

Analytical methods, sometimes referred to as deterministic methods, are amongst the most broadly used methodologies for BESS size determination. These methods are based on analyzing a series of power system configurations with the system elements varied being those that need to be optimized against performance criteria. Analytical methods are typically implemented by repetitive calculations or simulations performed over fixed intervals for the relevant system elements.

A study is developed by Ru et al. (2013), in order to size a grid-connected PV system for the purpose of power arbitrage and peak shaving. The electricity is generated from PV and is used to supply the demand from loads. The excess electricity generated can either be sold back to the grid or stored in a battery and electricity must be purchased from the electric grid if the PV generation and battery discharging cannot meet the demand. The objective is to minimize the cost associated with net power purchase from the electric grid and the battery capacity loss while at the same time satisfying the load and reducing the peak electricity purchase from the grid [72].

A novel is presented by Li et al. (2015), which analyzes the statistical properties and sizes the storage for wind-PV-storage hybrid systems that is based on the data organization.

The sized BESS is used to stabilize the power variance caused by fluctuating renewable energies and varying grid load [73].

In Yang et al. (2014), a strategy for sizing a battery energy storage is proposed in a distribution network with a higher PV penetration. The goal is to optimize the size of the distributed BESS and derive the cost-benefit analysis when the distributed BESS is applied for voltage regulation and peak load shaving [74].

4.1.3 Direct Search-Based Methods

An apparent refinement to analytical methods is to reduce the need for simulations across the entire configurational space of the system being analyzed in order to reach the optimal solution in a computationally efficient manner. There is a vast array of techniques developed for such optimization problems, including many being used for BESS sizing. These can be conventionally split into mathematical optimization techniques based on mathematical properties of the solution space, and heuristic techniques in which simple search parameters can be used to deliver an efficient algorithm, often based around nature inspired selection methods.

4.1.3.1 Mathematical optimization methods

The BESS sizing using mathematical optimization methods consists of the use of linear programming, mixed-integer programming or non-linear programming. Using such methods, an objective function is created and an interactive process is initialized and stops when the best results are reached. Other methods, such as Newton's method, descending gradient algorithm, and interior point algorithm, can be used to solve optimization problems. These methods can be resolved in a few steps, decreasing the computational effort. Furthermore, due to the relatively mature nature of these methods, professional software is available for solving optimization problems such as MATLAB toolbox and General Algebraic Modelling Systems (GAMS), amongst others. However, when the mathematical formulation increases their complexity, these tools face difficulties in converging to an optimum solution.

A model to select and optimally operate along with energy storage devices that were installed in a renewable generator integrated into the power system has been demonstrated in

[23]. The software LINDO is used to solve a mixed integer linear programming model in order to select the best energy storage system.

In Gao (2015), different energy storage system (ESS) sizing technologies are evaluated. An implementation of an expansion planning problem method for optimal storage sizing is proposed. The objective of this method is to minimize the operating cost, maintenance cost and investment cost of the entire micro-grid system. A case study is demonstrated, an optimization problem for determining both the optimal power rating and energy rating of ESS in a micro-grid is formulated and solved with mixed integer linear programming (MILP) [75].

A BESS sizing is proposed by Bahramirad et al. (2012) in a micro-grid considering reliability criterion. The ESS sizing problem is proposed which minimizes the investment cost of the ESS and the micro-grid cost. Mixed-Integer programming (MIP) is used to formulate the problem and its implemented using IBM ILOG CPLEX Optimization Studios (CPLEX) [76].

4.1.3.2 Heuristic methods

Heuristic methods allow non-optimal solutions that are sufficient for practical solutions. The main advantages are that they can avoid complicated derivatives, especially for non-linear optimization problems, thereby using reasonable memory and computational time.

Despite often having no mathematically proven basis for obtaining optimal solutions, heuristic approaches such as nature-inspired algorithms like Genetic Algorithms, Particle Swarm Optimization, artificial neural network, fuzzy logic, Tabu search, *etc*., tend to offer fast convergence, simple implementation and strong flexibility.

The authors Fossati et al. (2014), proposed a genetic algorithm to size an ESS in microgrids. The main goal of the proposed method is to find the energy and power capacities of the storage system that minimizes the operating cost of the microgrid. The energy management strategy used in this paper is based on a fuzzy expert system that is responsible for setting the power output of the ESS. In addition, the proposed method uses an aging model to predict the lifetime of the ESS. In this way, it is possible to determine the costs associated with energy storage in a more precise manner. The suggested sizing methodology has been validated in two case studies [77].

Tabu search is proposed by Chakraborty et al. to determine the optimal size of ESS integrated with a thermal power system. Tabu search is used to avoid re-evaluation of already evaluated ESS size, which is powered by max priority heap and hash table data structure. The

method proposed is applied in two different power systems in order to determine the appropriate size of the ESS [78].

As seen earlier, there have been a variety of techniques and approaches to solving the BEES sizing problem in a renewable energy system. Table 3 summarizes the previous methods cited, the implementation, advantages and disadvantages of sizing a BESS [65].

Table 3 - Summary of the advantages and disadvantages of BESS sizing.

Technique	Implementation	Advantages	Disadvantages
Probabilistic (depends on data resolution, more likely intra-hour, hourly data for a long duration	•Generates synthetic weather resources and PV/wind power generation data. •Generates synthetic scenarios for stochastic optimization.	•Overcomes the restriction of limited data availability. •Gives results with confidence levels.	•Accuracy relies on the availability of historical data. •May require computational extensive resources.
Analytical (Applications for optimization horizons ranging from repeated intra-hour simulations to several years of assessment)	•Direct calculation based on intuitive criteria. •Repeated computation/simulation with fixed intervals. •Sensitivity analysis.	•Better visualization with the change of battery sizes. •Strong flexibility for all criteria and simulation environments.	•Computationally intensive. •May miss global optimum if the data resolution is not high enough.
Mathematical optimization (Applications for hourly, intra-day or daily optimization)	•Linear, mixed-integer, quadratic programming problems. •Problems that can be linearized. •Problems that can be solved by numerical methods.	•Strong capability to finds the global optimum. •Fast convergence and high robustness for linear problems.	•High efficiency limited to linear/mixed-integer/quadratic programming problems. •Linearization may require extra derivations. •Explicit mathematical formulation required.
Heuristic (Applications for hourly, intra-day or daily optimization)	•Non-linear optimization problems. •Apply nature-inspired algorithms such as GA, PSO, Tabu search, and Bat algorithms.	•Strong flexibility to solve all optimization problems. •Avoid complicated derivatives. •Use less computational resources. •Simple implementation.	•May converge in local optimum instead of global optimum •Less robustness and accuracy for linear problems.

The technique that must be used for BESS sizing was analytical, and overall, technical indicators were the main factor in determining the size. In general, the BESS sizing in a renewable system can be seen to be a multi-faceted problem, involving single/multiple-objective optimization, decision-making and multiple systems simulation. In addition, the new research in advanced technologies continue worldwide. In this thesis, a BEES sizing is proposed in a PV using solar data for a given region. The BESS value showed the amount of energy necessary that a battery must have to provide constant power to the system under the uncertainties of a generation.

CHAPTER 5 - PROBLEM OUTLINE AND VARIABLES

With the rapid deployment of the energy storage system and the increasingly significant amount of variability introduced by the renewable generation are two of the most marked and exciting changes in the grids over the next few decades.

The modifications of the dynamic of the actual grid bring challenges and opportunities to the development of ESS technologies and control of the energy stored. In this way, the main objective of this thesis is sizing and the analysis of a BESS using the Conti-Varlet Technique to regularize the power provided to the grid.

The present thesis is divided into two main parts: the theoretical part and simulation part. The theoretical part is composed of a state of the art of the ESS with the objective to show the technologies already developed and new technologies and their functionalities and applicability. Also, the Conti-Varlet technique and its utilization in hydropower plants is shown, making an analogy to the ESS. The simulation part is the sizing of the ESS using the Conti-Varlet algorithm to regularize the power, as well the implementation of this model, conducting tests and analyzing the result. In this chapter, an introduction of distinct components and key assumptions will be discussed.

5.1. Solar Data

A case study in Itajubá, Brazil is presented. A PV farm with 140 m² of area (A) is considered. The solar data is obtained from the National Solar Radiation Data Base [79]. The required global solar irradiance (GHI) is the composition of the direct normal irradiation (DNI) along with the diffuse horizontal irradiance (DHI). These data are referred to as hourly irradiation of a sample year.

$$\mathrm{GHI} = \mathrm{DNI}\cos(\alpha) + \mathrm{DHI} \tag{16}$$

Where α is the solar zenith angle.

The daily output of a solar array depends on solar irradiation, solar cell temperature, and the operating point of the system. Irradiation is defined as the measure of the energy density of sunlight and is measured in W/m². Since energy is power integrated over time, irradiation is the integral of irradiance.

The data used are referred to as hourly radiation of a sample year. With these data, the studies of regularization already described are preceded as a basis for evaluation of battery power. The output power generated by the PV system is calculated by the following formula:

$$P_{pv} = \text{GHI} \cdot \eta_{pv} \cdot A \quad (17)$$

Where GHI [kW/m²] is the global horizontal irradiation at the location of solar panels, η_{pv} is the solar panels efficiency and A [m²] is the total area of solar panels. The expression 17 is a simplified version of the generation model and is not considered the temperature effect. If the temperature effect is considered, the generated power will be:

$$P_{pv} = (\text{GHI} \cdot \eta_{pv} \cdot A) \cdot [(1 + \alpha (T_C - T_{STC})] \quad (18)$$

Where α is the panel temperature coefficient, T_C is the panel temperature and T_{STC} is the nominal operating panel temperature. Table 4 presents the PV panel parameters [80]. The module SPR-305-WHT-D from SunPower [81] was chosen for the PV system. The stretched-thread method (STM) is implemented in the MatLab software.

Table 4 - PV System specifications.

Parameters	Value
Maximum PV power output (P_{pvmax})	305 W
Photovoltaic Panel Efficiency (η_{pv})	18.7 %
Rated Voltage (V_{mpp})	54.7 V
Rated Current (I_{mpp})	5.58 A
Open Circuit Voltage (V_{OC})	64.2 A
Short Circuit Current (I_{SC})	5.96 A
NOCT	45 °C
Negative Temperature Coefficient (ρ)	-2 °C

There are two types of the photovoltaic systems: the stand-alone PV system and grid-connected system. In a stand-alone system, the solar energy yield is matched to the energy demand. Solar energy produced often does not correspond in time with energy demand from connected loads; thus, a storage system is required. In a grid-connected system, the consumer can sell or buy energy for the utility. These cases were selected to evaluate the methodology and are discussed in sequence.

5.2. Minimization of Disutility

In an optimization problem, an objective function must be developed to establish problem restrictions. In this case, the objective is to minimize the electricity purchased from the utility; in other words, the disutility reduction provides the lowest BESS cost. In Figure 22, an example of analysis in a period of a year. The red area "A" indicates that the regulated power is above the load demand and sells the energy surplus (C_{SU}). On the other side, the green areas marked with "B" indicate that the regulated power is below the load demand that buy energy from the utility (C_{BU}).

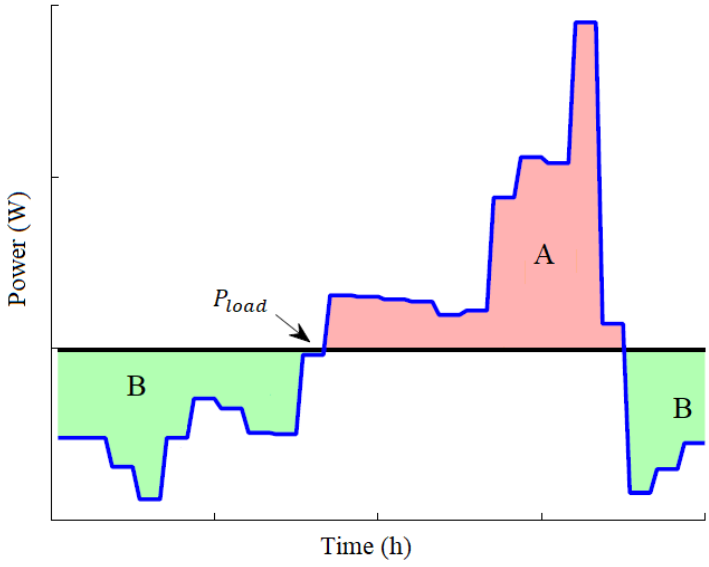

Figure 22 - Example of regularized power with a constant load.

Below the formulas for power surplus and power shortage for each regularized scenario are presented.

$$Area_A = P_{SU} = \sum_{i=1}^{T} \left(P_{Reg}(t) - P_{load} \right) \quad (19)$$

$$Area_B = P_{SH} = \sum_{i=1}^{T} \left(P_{load} - P_{Reg}(t) \right) \quad (20)$$

Where:

- P_{SU} is the electricity surplus from the BESS in time *t;*
- P_{SH} is the electricity shortage from the BESS in time *t;*
- P_{Reg} is regularized power in time t;

- P_{load} (t) is the load.

Expression 19 presents the amount of electricity that exceeds the demand and also the quantity of energy that the BESS can store while expression 20 is the total amount of electricity necessary to supply the load demand and charge the battery.

The optimization problem can be formulated by the following expression:

$$min_z = P_{SH} \,.\, C_{BU} \qquad (21)$$
$$P_{SH} \leq P_{load}$$

Where:

- C_{BU} is the cost of electricity purchased from the utility. An average value of 0.16 U$/kWh is considered;
- C_{SU} is the cost of electricity sold to the utility. An average value of 0.55 U$/kWh is considered;

It is considered that the energy is purchased from the utility at a low price and sold at a high price. The objective is to reduce the electricity purchased from the utility in the moments where electricity cannot be supplied by the PV and BESS. Some cases will be simulated, those being:

1°: The energy cost purchased from the utility in the period analyzed without the PV and battery system installed;

2°: The energy cost purchased from the utility in the period examined with the PV system.

3°: The energy cost purchased from the utility in the period analyzed with the BESS with different sizes;

In general, the steps will be described in Figure 23. As shown in Figure 23, the PV panels generate electricity which is consumed by the loads. On one hand, if there is an energy surplus, it can be stored in the BESS or sold to the utility. On the other hand, if there is not enough power to supply the demand, electricity will be purchased by the utility.

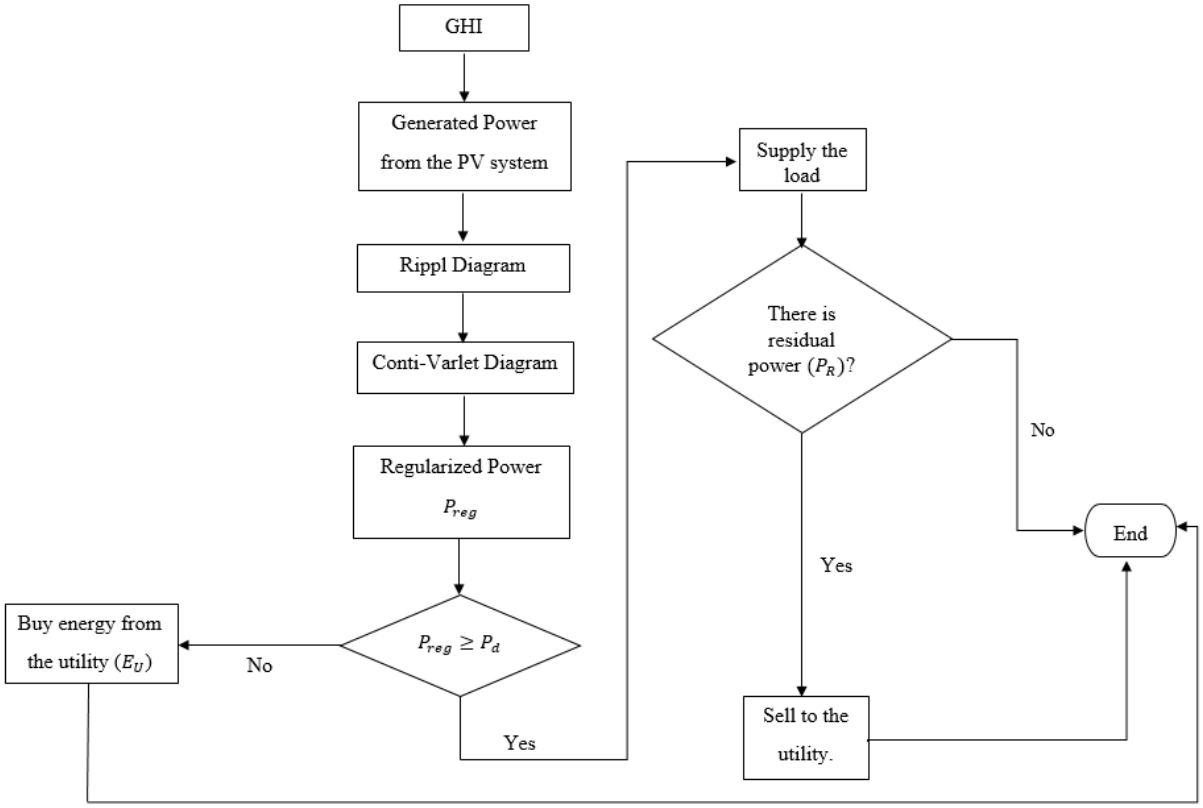

Figure 23 - Flowchart to the system logical operation.

In this thesis, different sizes of battery energy storage are being used to find the optimal size that reduces the disutility. The levelized cost of BESS is considered, of which the final energy price ($/MWh) is compounded by the investment costs, O&M and installation. To get the lowest disutility, three cases are simulated using linear programming. The method consists of obtaining the BESS that will provide the lowest value of energy purchased from the utility. The EES cost from battery technology is used from [82]. The value is shown in Table 5 from the year 2018.

Table 5 - Levelized Cost of a BESS.

BESS Technology	Price (US$/MW)		
	Min.	**Max.**	**Aver.**
Lithium	108	140	124

This value is very interesting because it reflects a real scenario of market competition. Also, the levelized costs internalize the initial investment required for construction of a PV plant plus the storage system.

5.3. Key Assumptions

The scope of this thesis is limited when considering all of the minor parameters that are not highly affected by the result of the optimization. While performing the key objective of minimizing the operational cost of the system, the process must keep some parameters as constants. All of those that considered assumptions and limitations have been described below.

- The BESS dynamic is not considered;
- The temperature in the PV panel is not considered;
- The load demand (P_{load}) is considered a constant at time *t*;
- The specific configuration of the necessary power electronics and its optimization are beyond the scope of the present work;
- Time of Use Tariff (TOU) is considered. The purchase price is assumed that the energy price is time [83] [84].
- The power flow on the grid is not considered.

CHAPTER 6 - STUDY CASE

In this chapter, the results will be discussed. In the first part of the chapter, a validation of the program developed and an application of the Conti-Varlet method are presented. In the second part of the chapter, a study case is taken into consideration. Based on the previously described Conti-Varlet method, the BESS will first be determined and then the optimal size of the BESS will be obtained. The results are obtained from the MatLab.

6.1. Benchmarking

A comparison between the results using the Stretched-Thread Method (STM) should be performed to evaluate its functionality and accuracy. In this way, a problem that uses the STM to regulate flow was taken into consideration. The developed program is tested in the data from [83]. A hydrogram with the normal flow and with the STM or Conti-Varlet technique applied in the Furnas reservoir is shown in Figure 24 and regularization is shown in Figure 25.

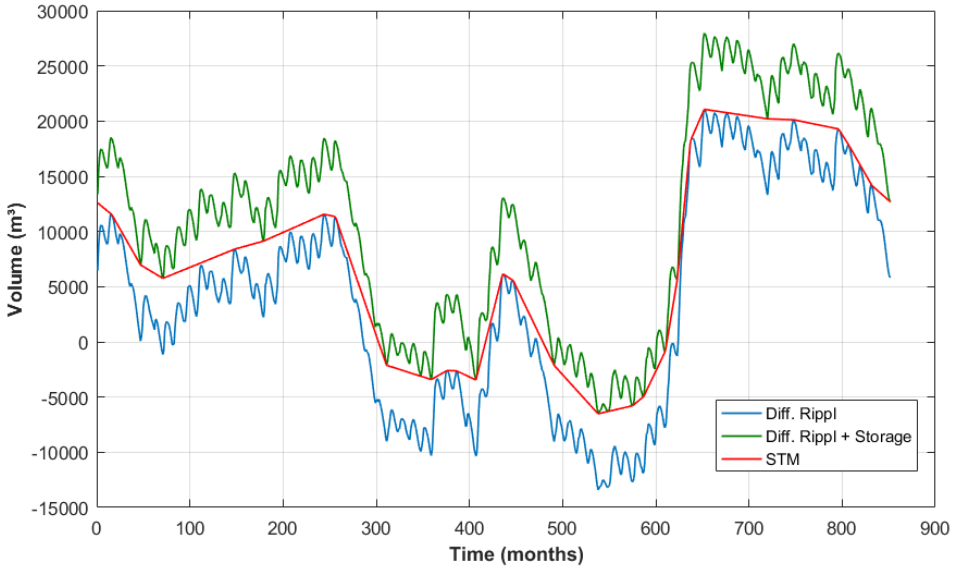

Figure 24 – Volume regularized from Furnas reservoir.
Source: *[83]*.

From [83], some important data can be obtained, such as the average flow of 932.59 m³/s and the average regularized flow of 917.96 m³/s. In this case, an error of 1.569% is obtained.

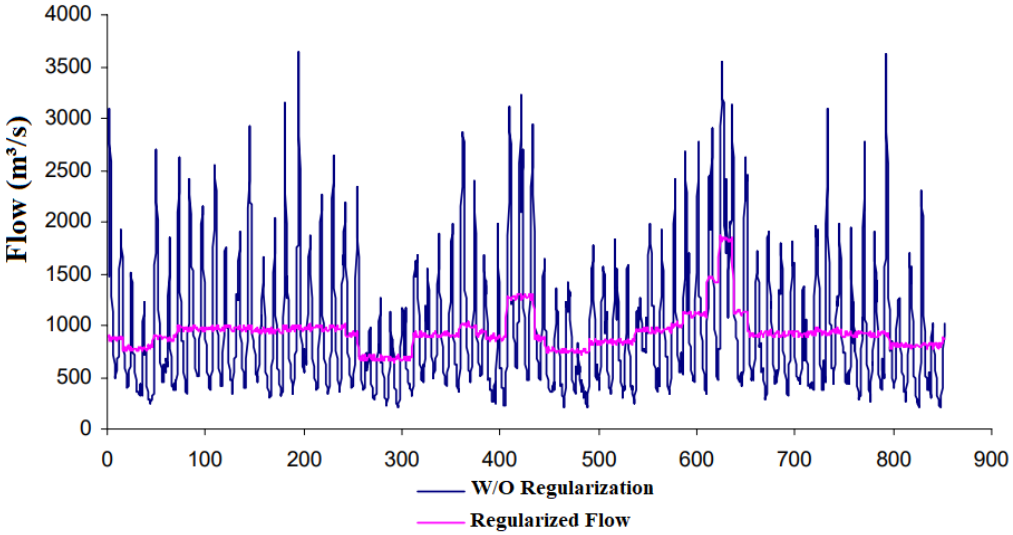

Figure 25 - Hydrogram of Furnas w/ and w/o regularization.

In applying the program developed in this thesis to the same problem, an average regularized flow of 931.819 m³/s and an error of 0.0826% is obtained. The method applied shows a satisfactory result and a better regulation. The regularized flow obtained is shown in Figure 26.

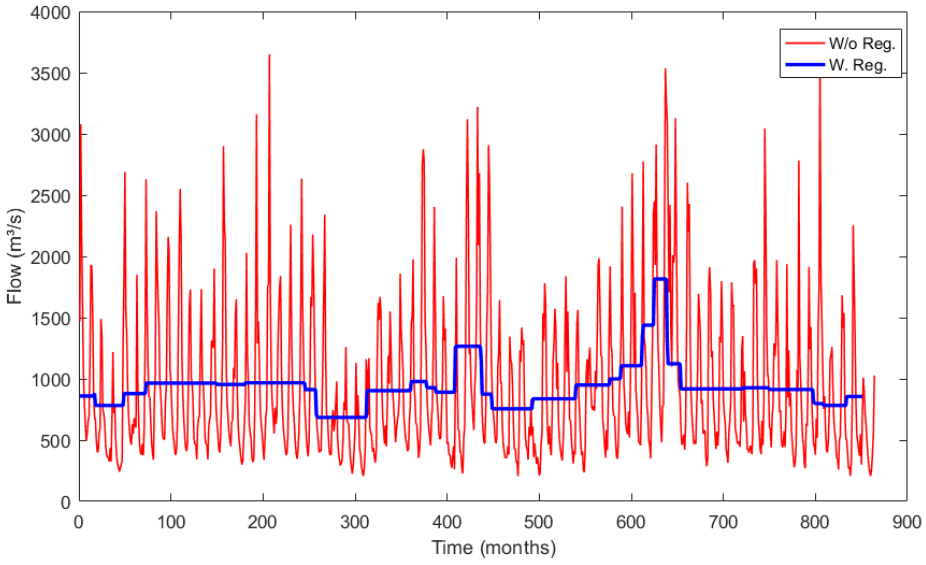

Figure 26 - Hydrogram of Furnas w/ and w/o regularization.

6.2. Conti-Varlet Method Application to Size a BESS

As presented in Chapter 3.3, the STM has the purpose of finding the most constant power possible. The first test realized is power regularization. Two scenarios for this test are simulated. In the first scenario, it is idealized as a situation when 20% of the power regularization is considered.

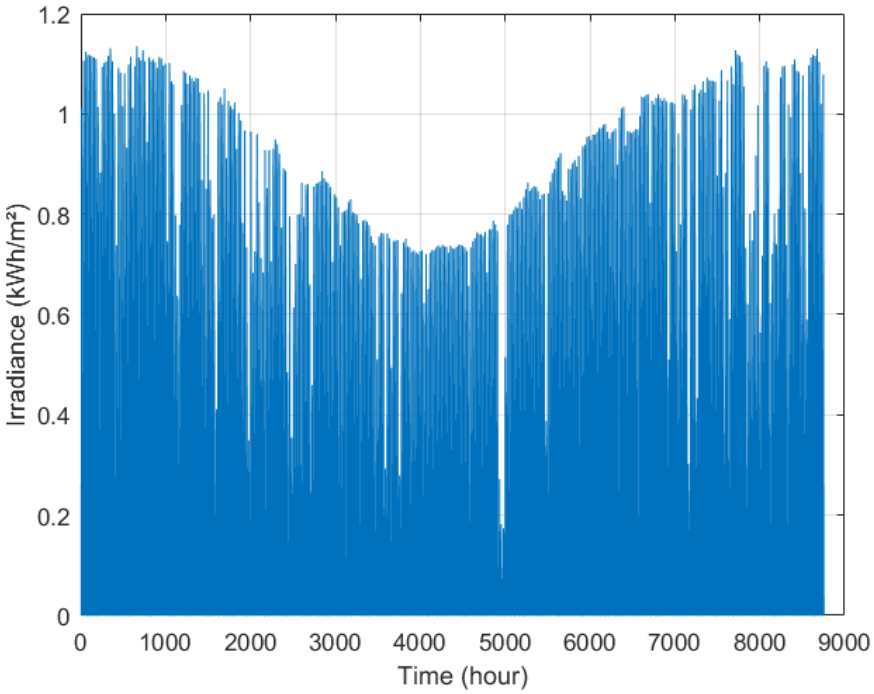

Figure 27 - Irradiance produced in a year.

The second scenario has proposed a regularization of 90%. The irradiance from yearly data is shown in Figure 27. It is expected that the load supply for several levels of regularization and the number of hours of operation will be obtained. The maximum value of power due to maximum irradiation is 212.45 W/m² and the annual average power is 45.97 W/m² are illustrated in Figure 28.

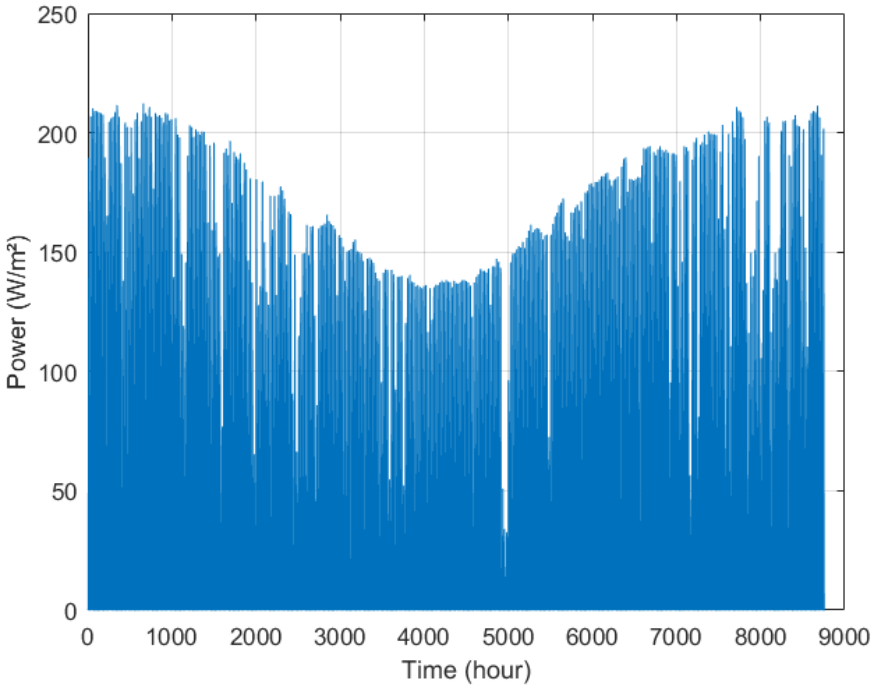

Figure 28 - Power available in a year.

Figure 29 depicts the Differential Rippl in which it is possible, from the maximum and minimum values, to obtain the BESS capacity to achieve total power regularization of 32.11 kWh/m².

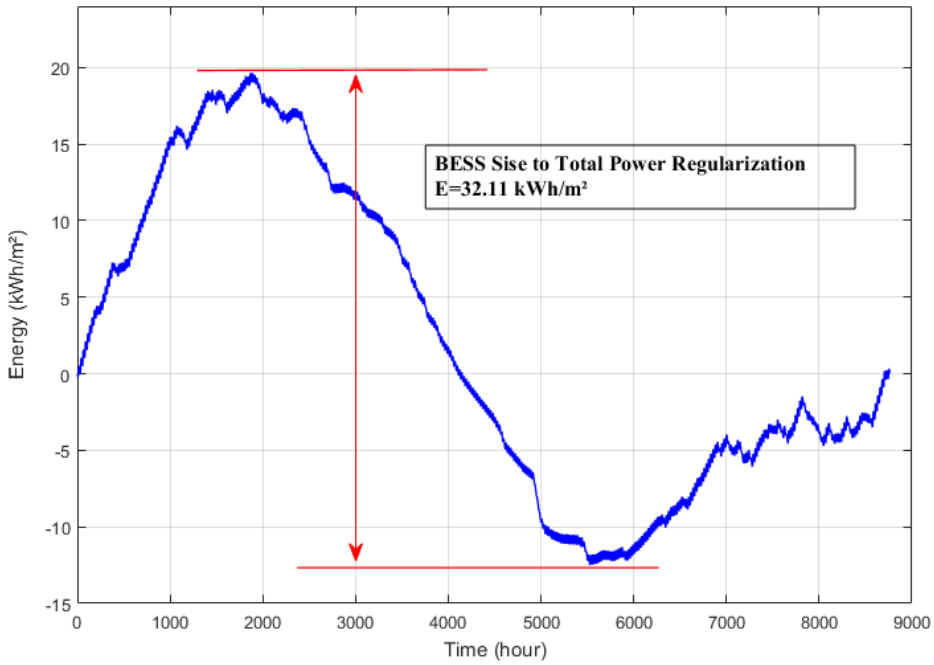

Figure 29 - Differential Rippl diagram.

Table 6 shows the battery capacity for each scenario of regularization (10-100%). In analyzing Table 6, it is possible to conclude that the more batteries installed in a given system, the more regularized the power will be. Nevertheless, an economic analysis will define the optimal size of the BESS.

Table 6 - BESS energy capacity for each regularization scenario.

BESS	10%	20%	30%	40%	50%	60%	70%	80%	90%	100%
(kWh/m²)	3.21	6.42	9.63	12.84	16.05	19.26	22.47	25.68	28.89	32.11

The Conti-Varlet diagram is the next step for power regularization. This consists of a Differential Rippl diagram added by the power provided for the BESS. Considering that 20% BESS is available to the system, then 6.42 kWh/m² should be added to the system. Figure 30 shows the Conti-Varlet diagram with 20% of the BESS capacity. A small gap between the Differential Rippl (E_R) and Differential Rippl+BESS (E_{DR}) was noticed. Likewise, these curve characteristics are due to the BESS size. In other words, lower desired regularization comes as a result of a lower storage level.

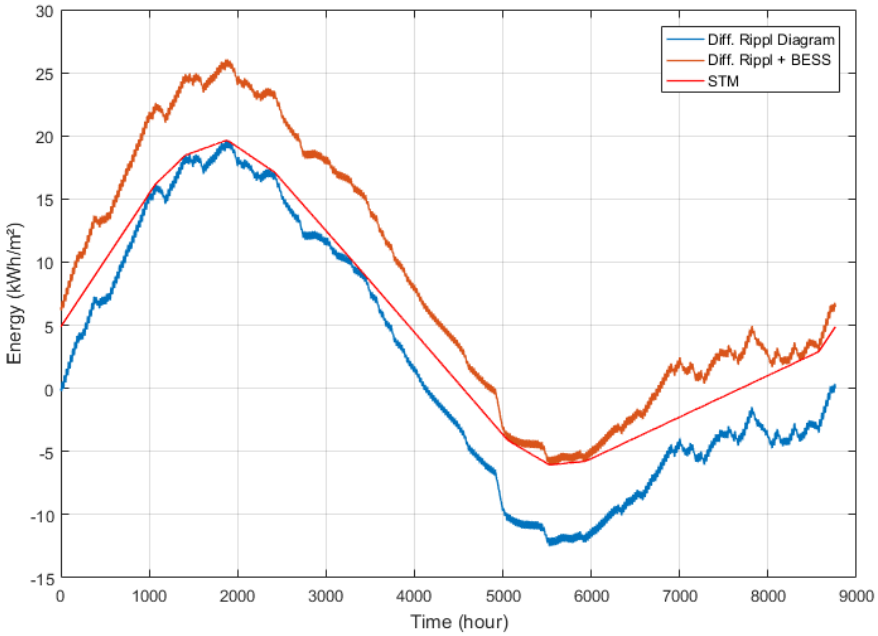

Figure 30 - Conti-Varlet diagram with 20% of total regularization.

Regularized power is shown in Figure 31. It is observed that the various steps on the curve happen because of the STM. In other words, due to small battery capacity, both curves will be closer, thus creating many intersection points for the STM.

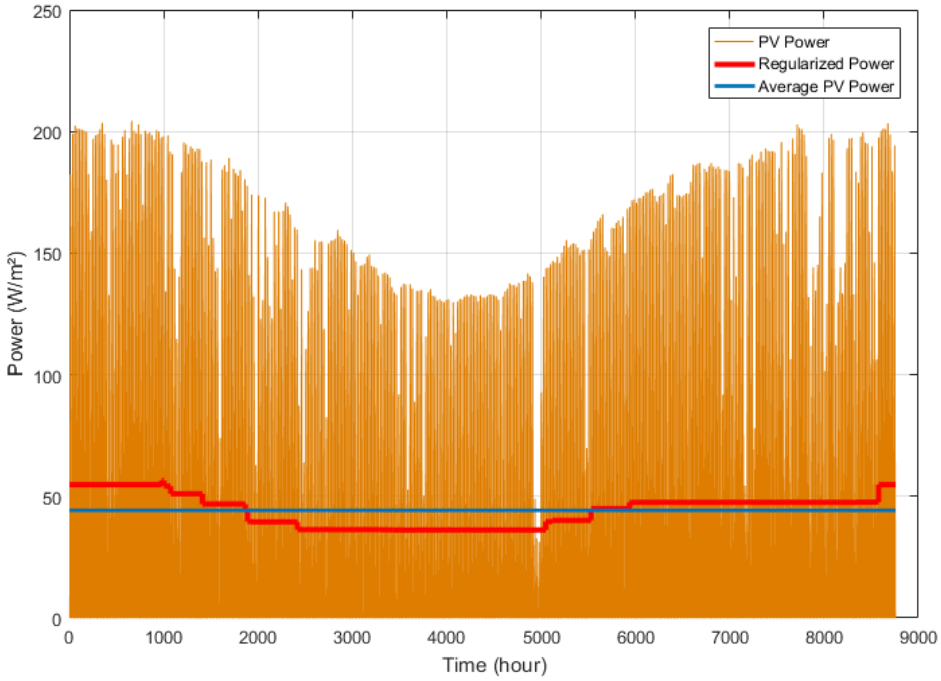

Figure 31 - Annual PV and regulated power (BESS=20%).

By increasing the BESS capacity to 90%, a battery capacity of 28.89 kWh/m² is added to the system. The Conti-Varlet diagram is changed in consequence and the energy regulated as shown in Figure 32.

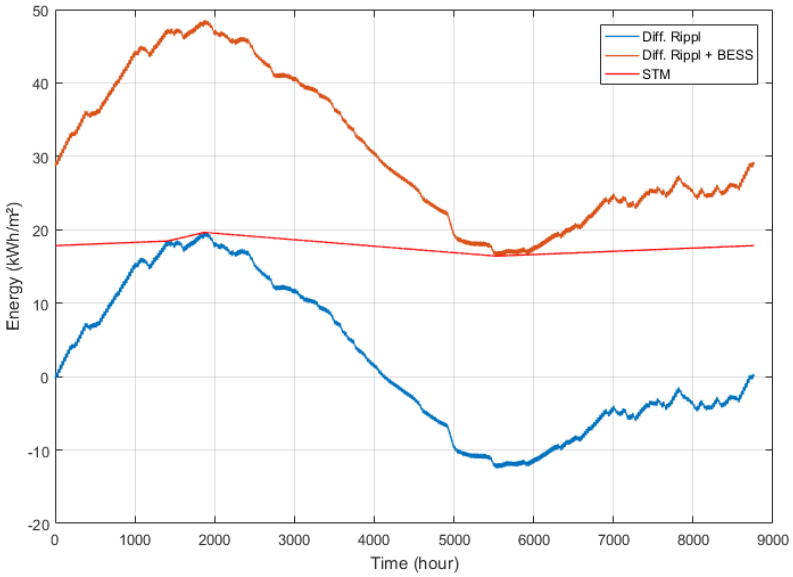

Figure 32 - Conti-Varlet diagram with 90% of battery capacity.

In Figure 33, a regularized power is shown. It is noticed that power value is almost constant. In this case, the BESS is regularizing almost all of the power available to the system

and the maximum power which can be regularized, or the total regularization is the average generated power to the system. Also, it shows the effect regularized achieved using the Conti-Varlet technique. The graphic obtained shows that when the power provided by the BESS is increased, the more regularized the power available will be due to consequently decreasing the drawbacks of the photovoltaic system. Also, through Varlet`s method, the regularized flow gets closer to the average flow.

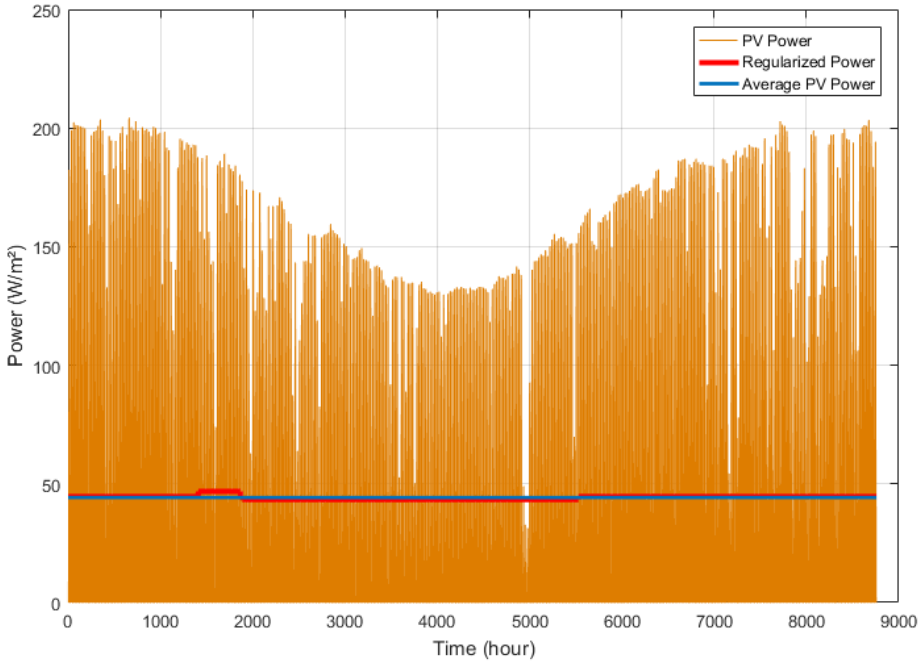

Figure 33 - Annual PV and regulated power (BESS = 90%).

In statistical terms, the more storage that is available in the system, the more the flow becomes regularized. In this way, the standard deviation will decrease in the same proportion. Also, this proves that the Conti-varlet diagram provides a constant flow in all periods that are higher or more constant in their intervals. As an example, the picture in Figure 34 shows the standard deviation of the regularized power as a function of the utile volume (storage capacity). In this case, 100% means a total regularization and the standard deviation is zero.

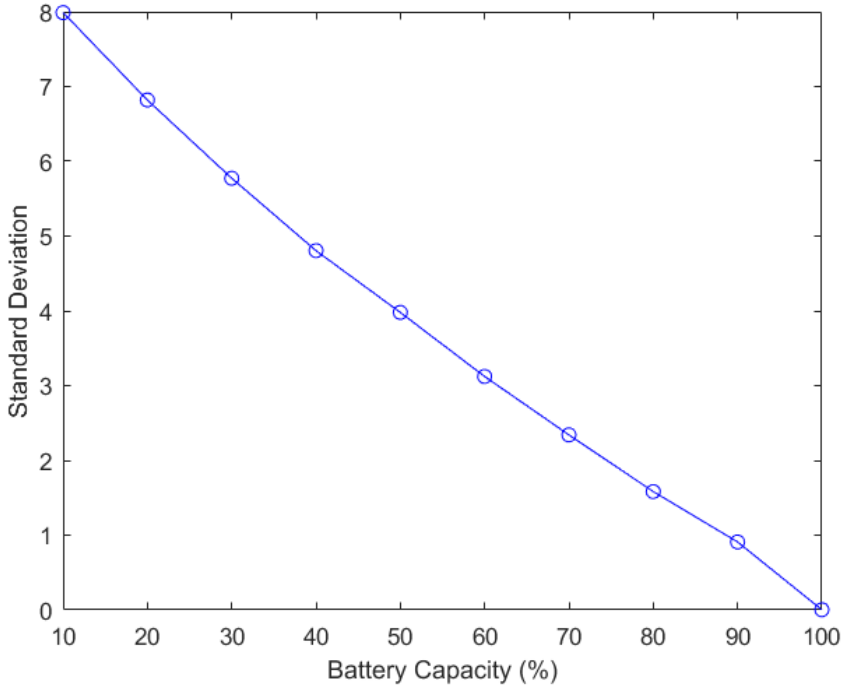

Figure 34 - Standard deviation of all regularization scenarios.

6.3. Disutility Optimization

The BESS sizing problem is an optimization problem whose objective is either to minimize the total micro-grid cost or to maximize the overall benefits. The BESS size is considered as a design variable whose optimal value is determined by solving an optimization problem. The proposed method size of a BESS has been applied in a fictional case, considering a PV plant of 140 m² and the load demand has been set to approximately 4315.2 kWh-monthly. These values were chosen so that the average generated power is the same or close to the average energy consumed by the residence.

6.3.1. Grid-connected PV system

Grid-connected photovoltaic systems are composed of PV arrays connected to the grid through a power conditioning unit and are designed to operate in parallel with the electric utility grid. In this case, all of the energy surplus or energy deficit are negotiable with the utility.

6.3.1.1. Energy consumed only by the utility

In this scenario, the system is compounded only by the loads and the electricity is exclusively provided by the utility in order to attend the demand. The total energy consumed in a year will be approximately 50,808 kWh-year and the cost associated with it is 812,928.00 US$.

6.3.1.2. Energy consumed by the utility and PV system

In this situation, a PV system with 19.2 kW of peak is added to the system. The average cost associated with this PV system is US$ 25,563.64 [84]. The $E_{PV\_monthly}$ shows the average power provided by the PV system for each month. E_{SU} and E_{SH} are the energy surplus and shortage respectively. The community has an average demand of 4315,2 kWh per month. Table 7 shows the average power consumed, the power surplus and the power deficit.

Table 7- Monthly output/load balance for PV installation.

Month	$E_{Avg\_monthly}$	$E_{PV\_monthly}$	E_{SU} or E_{SH}
January	4315.20	6104.25	1789.05
February	3897.60	5208.99	1311.39
March	4315.20	4494.24	179.04
April	4176.00	3732.75	-443.25
May	4315.20	3739.60	-575.60
June	4176.00	3378.14	-797.86
July	4315.20	3417.57	-897.63
August	4315.20	4406.27	91.07
September	4176.00	4926.47	750.47
October	4315.20	5021.28	706.08
November	4176.00	4654.19	478.19
December	4315.20	5195.64	880.44
Total (year)	**50808.00**	**54279.39**	**3471.39**

It is evident from the calculation presented in Table 7 that over an average year, the system would produce a good amount of surplus energy, a total of 6185.73 kWh/year to be exact. On the other hand, a deficit of 2714.34 kWh/year would also accrue. These values can be associated with their purchase and sales costs. The profit obtained for this case is 2967.87 US$ per year. Considering that all surplus energy is sold to the utility, in this analysis it was noticed that there was a deficit of four months on the power generation due to the characteristics

of irradiance in this period of the year. Consequently, being necessary to purchase energy from the utility in those periods.

6.3.1.3. The energy purchased from the utility with PV+BESS

In this section, all of the regulations (10-100%) are simulated to obtain the battery capacity for each scenario. Two values of BESS are taken into consideration and these values are obtained from the percentage of the total storage capacity from total regularization. These values are shown in Table 8.

Table 8 - Battery energy storage capacity.

BESS	10%	20%	30%	40%	50%	60%	70%	80%	90%	100%
(MWh)	**0.45**	**0.9**	**1.35**	**1.8**	**2.25**	**2.7**	**3.15**	**3.6**	**4.05**	**4.49**

Two values for the storage size have been selected, and they are expressed as a percentage of the total regularization. These values are 0.9 MWh, and 4.05 MWh and their effect on the regularization is shown in Figure 35 and Figure 36, respectively. As discussed in Chapter 5.2, the regularization will be analyzed in the context of two different conditions: selling energy when the system is generating or has stored more energy than necessary to supply the load with the regularization or purchasing energy from the utility when the regularized power is unable to supply all of the demand. The diagram was realized from a year analysis and a discussion is to follow.

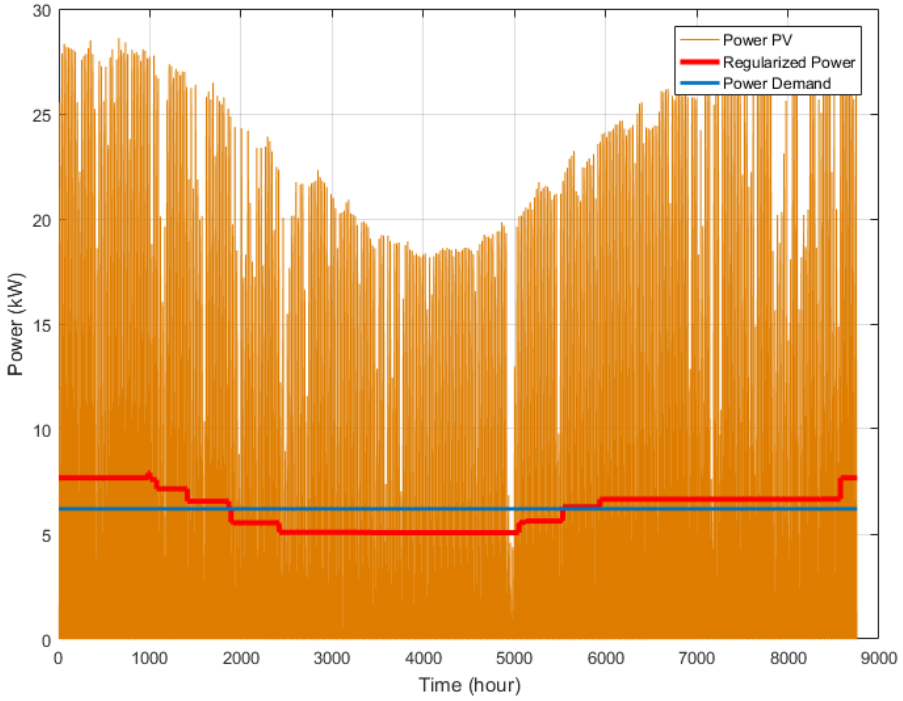

Figure 35 - Regularization effect with 20% of BESS.

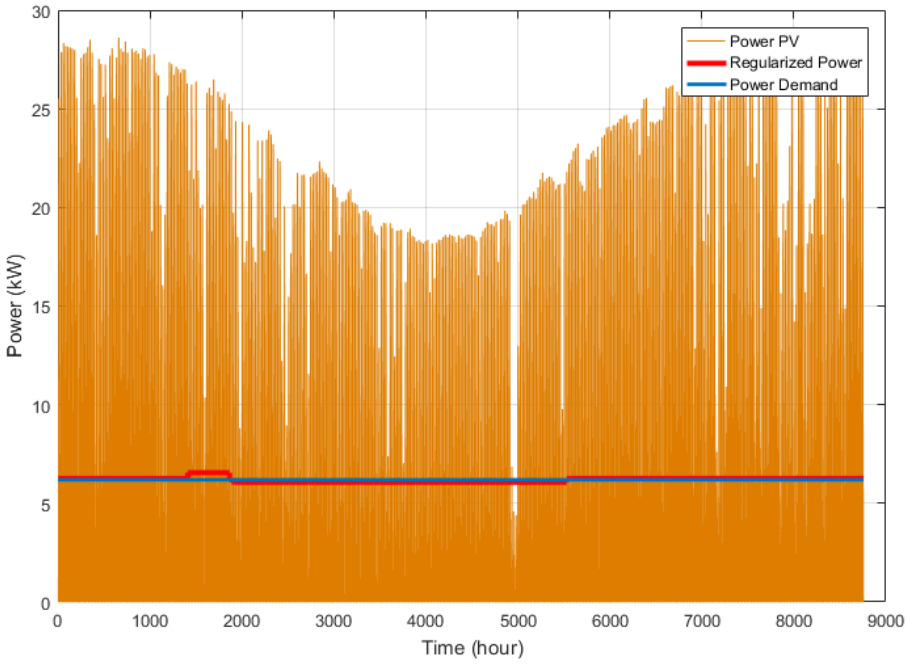

Figure 36 - Regularization effect with 90% of BESS.

As can been seen with more storage in the system, more regulated will the power delivered to the consumer be. This has been proven by Varlet's method. In order to quantify the regularized power, the values are converted in average energy monthly values. These conversions are applied to both regularized power and power demand in order to calculate the

benefits of the regularization. The economic benefit of using the regularization is mainly of reducing the dependency of the utility and reduce the drawback of the intermittence generation. Several factors influence the costs of the PV system and the storage system, such as installation and maintenance. In order to determine the ideal balance between storage size and cost, the energy consumption from the entire year must be taken into consideration. In Table 8, the average energy demand for each month is shown along with a regularized energy and the energy shortage and surplus. At the bottom of the table, a cost is applied for the energy surplus and deficit. Through the table, it is observed that the battery that provided the most significant profit in annual value is with 10% of regularization and a battery of 0.9 MWh. On the other hand, the regularization with the lowest income is how 100% of the regularization is expected, or the highest storage system with a capacity of 4.49 MWh due to the fact presented by Varlet`s Method. Some discussion can be inferred about these results from Table 9. In the first scenario with 10% of regularization, some periods of the year (April to July) present a negative value between the demand and the

Table 9 – Results obtained from the regularization to each scenario (part1).

Month	E_D (kWh)	BESS 10%		BESS 20%		BESS 30%		BESS 40%		BESS 50%		BESS 60%	
		E_{Reg}	E_{SU} or E_{SH}	E_{Reg}	E_{SU} or E_{SH}	E_{Reg}	E_{SU} or E_{SH}	E_{Reg}	E_{SU} or E_{SH}	E_{Reg}	E_{SU} or E_{SH}	E_{Reg}	E_{SU} or E_{SH}
January	4315.20	5994,59	1679,39	5706,44	1391,24	5428,31	1113,11	5175,01	859,81	4938,66	623,46	4889,78	574,58
February	3897.60	5058,24	1160,64	4971,66	1074,06	4869,48	971,88	4736,29	838,69	4631,45	733,85	4416,46	518,86
March	4315.20	4596,51	281,31	4596,52	281,32	4596,52	281,32	4596,52	281,32	4607,18	291,98	4642,22	327,02
April	4176.00	3769,10	-406,89	3774,64	-401,36	3842,41	-333,59	3921,33	-254,67	4006,87	-169,13	4099,50	-76,50
May	4315.20	3723,01	-592,18	3775,54	-539,66	3898,56	-416,64	4025,66	-289,54	4146,20	-169,00	4242,04	-73,16
June	4176.00	3444,31	-731,68	3644,88	-531,12	3772,80	-403,20	3895,80	-280,20	4012,45	-163,55	4105,20	-70,80
July	4315.20	3588,88	-726,31	3785,27	-529,93	3910,52	-404,68	4030,96	-284,24	4146,20	-169,00	4242,04	-73,16
August	4315.20	4382,81	67,61	4382,81	67,61	4382,81	67,61	4382,81	67,61	4383,67	68,47	4421,05	105,85
September	4176.00	4877,88	701,88	4754,81	578,81	4754,81	578,81	4754,81	578,81	4955,82	779,82	4702,94	526,94
October	4315.20	5031,40	716,20	4952,43	637,23	4952,43	637,23	4952,43	637,23	4938,66	623,46	4889,78	574,58
November	4176.00	4678,38	502,38	4792,67	616,67	4792,67	616,67	4792,67	616,67	4779,35	603,35	4732,04	556,04
December	4315.20	5118,07	802,87	5139,57	824,37	5070,78	755,58	5008,14	692,94	4932,02	616,82	4883,21	568,01
		Cost Sell	3251.77	**Cost Sell**	3009.22	**Cost Sell**	2762.22	**Cost Sell**	2515.19	**Cost Sell**	2387.67	**Cost Sell**	2063.53
		Cost Buy	393.13	**Cost Buy**	320.33	**Cost Buy**	249.30	**Cost Buy**	177.38	**Cost Buy**	107.31	**Cost Buy**	46.96
		Profit (year)	**2858.64**	**Profit (year)**	**2688.89**	**Profit (year)**	**2512.92**	**Profit (year)**	**2337.81**	**Profit (year)**	**2280.36**	**Profit (year)**	**2016.55**

Table 9 - Power Regularization to each scenario (part 2).

Month	E_D (kWh)	BESS 70%		BESS 80%		BESS 90%		BESS 100%	
		E_{Reg}	E_{SU} or E_{SH}	E_{Reg}	E_{SU} or E_{SH}	E_{Reg}	E_{SU} or E_{SH}	E_{Reg}	E_{SU} or E_{SH}
January	4315.20	4810,81	495,61	4731,85	416,65	4655,40	340,20	4609,51	294,31
February	3897.60	4345,77	448,17	4275,09	377,49	4206,65	309,05	4163,43	265,83
March	4315.20	4675,81	360,61	4709,39	394,19	4742,98	427,78	4615,60	300,40
April	4176.00	4188,28	12,28	4277,07	101,07	4365,85	189,85	4454,62	278,62
May	4315.20	4333,91	18,71	4425,78	110,58	4517,66	202,46	4609,51	294,31
June	4176.00	4194,11	18,11	4283,02	107,02	4371,92	195,92	4460,82	284,82
July	4315.20	4333,91	18,71	4425,78	110,58	4517,66	202,46	4609,51	294,31
August	4315.20	4475,62	160,42	4530,00	214,80	4573,75	258,55	4609,51	294,31
September	4176.00	4637,43	461,43	4572,13	396,13	4505,23	329,23	4460,82	284,82
October	4315.20	4810,81	495,61	4731,85	416,65	4655,40	340,20	4609,51	294,31
November	4176.00	4655,63	479,63	4579,21	403,21	4505,23	329,23	4460,82	284,82
December	4315.20	4810,81	495,61	4731,85	416,65	4655,40	340,20	4609,51	294,31
		Cost Sell	1905.71	**Cost Sell**	1905.77	**Cost Sell**	1905.82	**Cost Sell**	1905.86
		Cost Buy	0	**Cost Buy**	**0**	**Cost Buy**	**0**	**Cost Buy**	**0**
		Profit (year)	**1905.71**	**Profit (year)**	**1905.77**	**Profit (year)**	**1905.82**	**Profit (year)**	**1905.86**

regularized values. These negative values are due to the lack of PV generation as well as the low regularization. Thus, with a small storage system, the energy consumption by the utility would be evident. In this case, the energy purchase in these periods (dry periods) would have a high cost. However, when more storage is added to the system, the regularized power increases with the values approaching the average generation power being the value of load demand. In this case, the energy storage capacity will provide a power value that will pursue the average power generation defined by the Varlet's method of the minimization of the standard deviation. With total regularization, the consumer will not buy energy from the consumer. In this case, there is no disutility. On the other hand, the consumer will also have the lowest energy surplus value, thus generating the smallest revenue in comparison to the different regularization scenarios. Figure 37 presents the relationships between the increase the regularization and profit for energy surplus and deficit.

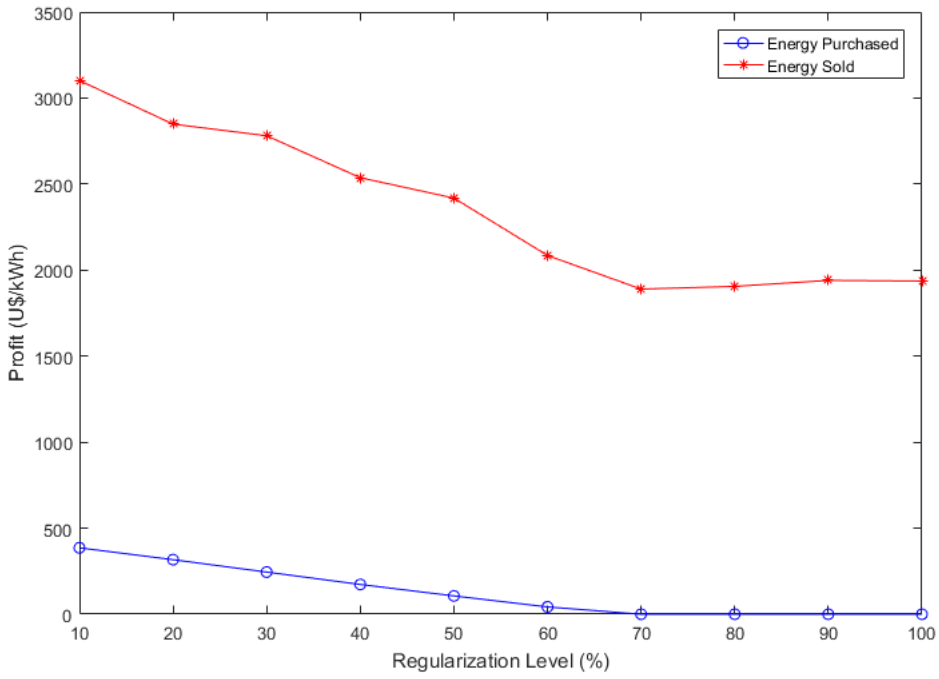

Figure 37 - Energy profit reduction for each regularization scenario.

In order to examine the impact of ESS size on the total cost of the micro-grid, the optimization problem is resolved with all of the battery sizes. Table 10 shows that for each scenario of regularization (10-100%) the battery capacity and also the BESS costs associated with all of the energy storage capacity applied in this work.

Table 10 - Energy Storage Costs for different battery technologies.

	Energy Storage Costs (US$/MWh)									
BESS	**10%**	**20%**	**30%**	**40%**	**50%**	**60%**	**70%**	**80%**	**90%**	**100%**
(MWh)	0.45	0.90	1.35	1.80	2.25	2.70	3.15	3.60	4.05	4.49
1	55.74	111.47	167.21	222.94	278.68	334.41	390.15	445.88	501.62	557.35

With the values presented in Table 10 it is possible to create a graph that shows the associated costs of different battery sizes and technologies, as depicted in Figure 31. As can be seen in Figure 31, the ESS investment cost increases linearly as the energy and the regularized power ratings of the BESS increase. A greater size of the BESS can store more energy at off-peak hours and thus produce more energy at peak hours, which provides higher economic benefits for the micro-grid system. However, for a 0.45 MWh BESS, it is the best cost-benefit scenario due to the profit obtained in a one-year analysis. It is clear that for each regularization scenario, there is a different energy rating value for the BESS and with more battery, more constant will the power delivered to the customer be while being of the lowest disutility.

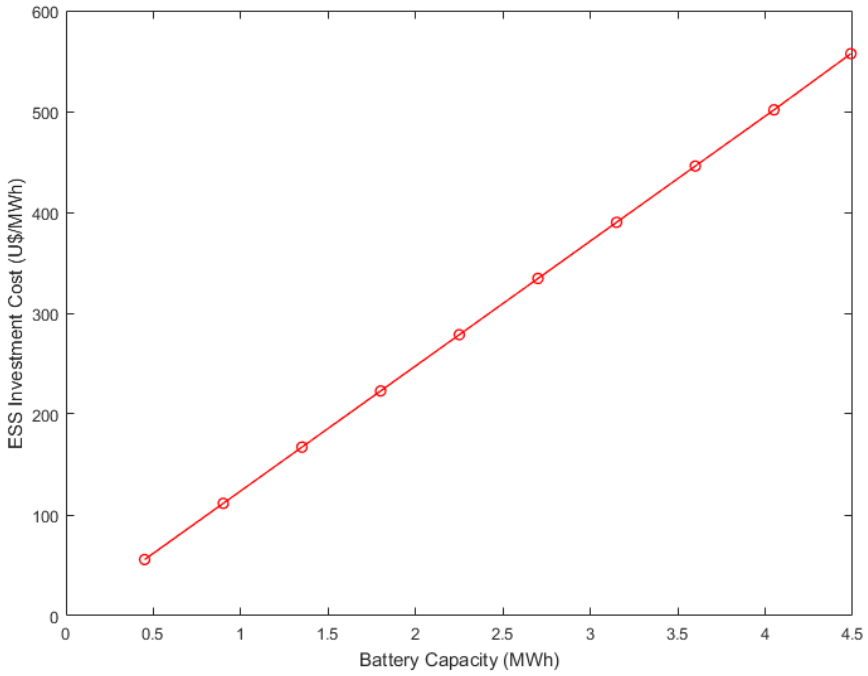

Figure 38 - ESS investment cost at different regularization scenarios.

CHAPTER 7 - CONCLUSION

This thesis presented the application of proven technology for hydropower plants applied to solar power plants. In this case, the battery was compared to the reservoir resulting from a dam. Some case studies were performed. The effect of the battery comes with the Conti-Varlet technique, relocating the Differential Rippl diagram and finding the straight lines between upper and lower limits. Varlet's technique proves to be an accurate method for sizing a storage system. However, Varlet's method has its own restraints, causing a conflict in the optimization. The main problem occurs in the STM when the simulation chooses the shortest path between the graphs. When the graph reaches the upper curve, the battery is fully charged or charging, and when reaching the lower curve, the battery is discharged or discharging. Those periods of charge and discharge are automatically generated by Varlet's method and make it impossible to store the surplus energy in a period of higher generation and sell or use it in a period of lower generation.

In order to evaluate an ESS, a methodology should consider diversity in location and application, ownership, operation, control models, local information on regulation, tariffs, market rules, climate, *etc*. These methodologies need high-fidelity operational visibility to capture reciprocity between devices and their applications considering the current modern and complex electrical network; they also require a complex evaluation system in order to calculate the impacts.

In relation to the optimization model developed through its application, it is observed that, although simplistic, it behaves as expected in view of the objectives of this dissertation. The problem applied was easy to solve since it was considered data with certainty of supply; for a real application would require a greater number of examples to be analyzed in order to obtain a safer projection of the operation of the storage system.

A consideration to be made about the results of the simulations is that they were heavily influenced by standardized costs of energy provided by Lazard [82]. Renewable energy sources, mainly wind and solar, have gained market and scale, and thus the US$/kWh installed has been decreasing year after year even with deployment and operating costs being more attractive than nuclear source and sources using fossil fuels such as coal, shale or natural gas to generate energy. However, renewable energy generation is intermittent and does not have the ability to track demand. When inserting a BESS to the system, these disadvantages are reduced or mitigated.

In conclusion, the proposed technique proved to be adequate for intermittent generation. For example, with the photovoltaic generation, the method can be used in other sources such as wind. The important thing is to have the data of the locale of interest. It could be interesting for future work to calculate the optimal BESS size to reduce the disutility and in doing so use different ESS to determine which technologies offer superior operation at lower costs.

7.1 Future Works

In order to fully determine that this new approach of Varlet's method is accurate to size a BESS or other storage technologies, more data should be added along with a benchmark with other sizing methodologies being performed.

For this research, the simulation model has been built but the battery dynamic was not considered. This should be incorporated in order to validate the battery sizing strategy. The sizing method used in this research is a basic starting point for a new approach in sizing batteries and can be incorporated in larger storage system and other storage technologies.

An online dispatch of the energy stored with dynamic pricing considering the cloud prevision in a photovoltaic system is an exciting tool for system planning

REFERENCES

[1] D. Sandoval, P. Goffin and H. Leibundgut, "How low exergy buildings and distributed electricity storage can contribute to flexibility within the demand side," *Applied Energy, Vol. 87,* pp. 116-127, February 2017.

[2] REN21, "Renewables 2018 Global Status Report," 2018.

[3] WEC - World Energy Council, 2016. [Online]. Available: https://www.worldenergy.org/data/resources/resource/wind/. [Accessed 23 november 2017].

[4] MME, "Ministério de Minas e Energia. Boletim mensal de monitoramento do setor elétrico - dezembro de 2016.," 2017.

[5] "Terra," 13 June 2018. [Online]. Available: https://www.terra.com.br/noticias/dino/brasil-ultrapassa-15-gw-de-energia-solar-fotovoltaica-e-abastece-mais-de-633-mil-residencias,dd2895195bcd436bcf6b57cf2b328a44z1o95kjd.html. [Accessed 15 June 2018].

[6] F. D. Gonzalez, A. Sumper and O. G. Bellmunt, Energy Storage in Power Systems, Barcelona, Spain: Wiley, 2016.

[7] A. Gautier, J. Jacqmin and J. C. Poudou, "The Prosumers and the Grid," *International Industrial Organization Conference,* p. 32, November 2017.

[8] J. S. Hill, "Clean Technica," 22 november 2017. [Online]. Available: https://cleantechnica.com/2017/11/22/navigant-research-identifies-1700-energy-storage-projects/. [Accessed 23 november 2017].

[9] F. A. Farret, "Integration of Alternative Sources of Energy," *John Wley & Sons,* pp. 262-295, 2017.

[10] I. A. Raihan, "Impact of Energy Sorage Devices on Relibility of Distribution System," *2nd International Conference on Electrical,Computer & Telecommunication Engineering (ICECTE),* 2016.

[11] P. P. Barker and R. W. De Mello, "Determining the impact of distributed generation on power systems. I. Radial distribution systems," *2000 Power Engineering Society Summer Meeting* , p. 12, 16-20 July 2000.

[12] A. H. M. Santos, "Uma versão computacional do método de Conti-Varlet para estudos de regularização parcial de vazões em pequenas e médias bacias.," *Simpósio Brasileiro de Recursos Hidrícos, ABRH 4,* p. 11, 1993.

[13] "Sola Photovoltaic Technology Basics," NREL - National Renewable Energy laboratory, [Online]. Available: https://www.nrel.gov/workingwithus/re-photovoltaics.html. [Accessed 04 June 2018].

[14] R. Messenger and A. Abtahi, Photovoltaic systems Engineering, USA: CRC Press, 2017.

[15] A. A. Akhil, G. Huff, A. B. Currier, B. C. Kaun, D. M. Rastler, S. B. Chen, A. L. Cotter, D. T. Bradshaw and W. D. Gauntlett, "DOE/EPRI 2013 Electricity Storage Handbook in Collaboration with NRECA," p. 163, 2013.

[16] P. A. Ribeiro, B. K. Johnson, L. C. Mariesa, A. Arsoy and Y. Liu., "Energy Storage Systems for Advanced Power Applications," *Proceedings of the IEEE, vol.89, No. 12*, 2001.

[17] P. Denholm, E. Ela, B. Kirby and M. Milligan, "The Role of Energy storage with Renewable Electricity Generation," NREL - National Renewable Energy Laboratory, Golden, Colorado-USA, 2010.

[18] Deloitte & Touche LLP, "Energy storage: Tracking the technologies that will transform the power sector.," 2015.

[19] ESA, "Grid Operations Benefits," Energy Storage Association, 2018. [Online]. Available: http://energystorage.org/energy-storage/energy-storage-benefits/benefit-categories/grid-operations-benefits. [Accessed 19 May 2018].

[20] AESA - Alberta Electric System Operator, "Energy Storage Integration," 2015.

[21] M. G. Molina, "Energy Storage and Power Electronics Technologies: A Strong Combination to Empower the Transformation to the Smart Grid," *Proceeding of the IEEE*, p. 29, 10 February 2017.

[22] B. F. Nunes, Y. F. F. C. Silva and E. C. Bortoni., "Optimized selection and operation of electrical energy storage systems.," *IEEE Power & Energy Society General Meeting*, 2015.

[23] Y. F. F. Costa e Silva, "Um modelo para seleção e operação otimizada de sistemas de armazenamento de energia elétrica em redes inteligentes," in *Master degree thesis*, Itajubá, 2016.

[24] Institute, EPRI - Electric Power Research, "Electricity Energy storage Technology Options: A white paper Primer on Applications, Costs, and Bnefits.," EPRI, Palo Alto, CA, 2010.

[25] H. Alharbi, "Optimal Planning and Scheduling of Battery Energy Storage Systems for Isolated Microgrids," in *University of Waterloo*, Ontario, Canada, 2015.

[26] "Electrical energy storage, Commission, Int. Electrotech.," in *White Paper*, Geneva, Switzerland, 2011.

[27] H. Chen, T. N. Cong, W. Yang, C. Tan, Y. Li and Y. Ding, "Progress in electrical energy storage system: A critical review," *Prog. Natural Sci., vol. 19, no. 3,* p. 291–312, 2009.

[28] I. Alsaidan, A. Khodaei and W. Gao, "A Comprehensive Battery Energy Storage Optimal Sizing Model for Microgrid Applications," *IEEE Transactions on Power Systems,* p. 13, 3 november 2017.

[29] WEC - World Energy Council, "World Energy Resources: E-storage: Shifting from cost to value Wind and solar applications," London, 2016.

[30] M. Welsch, "Europe´s Energy Transition: Insights for Policy Making," p. 354, 19 April 2017.

[31] " ERRA-Energy Regulators Regional Association, Pumped Storage Hydroelectric Power Plants: Issues and Applications," 2016.

[32] " U.S. Dep. Energy, Global energy storage database," Tech. Rep, Washington, DC, USA, 2017.

[33] G. Fuchs, B. Lunz, M. Leuthold and D. U. Sauer, "Overview on the potential and on the deployment perspectives of electricity storage technologies," ISEA , 2012.

[34] "Pollegio-Loderio Tunnel ALACAES Demonstration Plant," DOE - GLOBAL ENERGY STORAGE DATABASE, 19 may 2016. [Online]. Available: https://www.energystorageexchange.org/projects/1355. [Accessed 17 november 2017].

[35] H. Ibrahim, A. IIinca and J. Perron, "Energy storage systems—Characteristics and comparisons," *Renew. Sustain. Energy Rev.,vol. 12, no. 5,* p. 1221–1250, 2008.

[36] X. Luo, J. Wang, M. Dooner and J. Clarke, "Overview of current development in electrical energy storage technologies and the application potential in power system operation," *Applied Energy, Volume 131,* pp. 511-536, 1 January 2015.

[37] R. Peña-Alzola, R. Sebastián, J. Quesada and A. Colmenar, "Review of flywheel based energy storage systems," *Proc. Int. Conf. Power Eng., Energy Elect. Drives,* pp. 1-6, May 2011.

[38] B. R. Chalamala, R. Guttromson and R. D. Masiello, "Energy storage—Part II: Realizing the value," *Proc. IEEE, vol. 102, no. 7,* p. 1050–1051, July 2014.

[39] P. P. Barker, "Ultracapacitors for use in power quality and distributed resource applications," *Proc. IEEE Power Eng. Soc. Summer Meeting,* p. 316–320, July 2002.

[40] S. Wang, T. Wei and Z. Qi, "Supercapacitor Energy Storage Technology and its Application in Renewable Energy Power Generation System," *Proceedings of ISES World Congress 2007 (Vol. I – Vol. V)* , pp. 2805-2809, 2007.

[41] K. E. Nielsen and M. Molinas, "Superconducting magnetic energy storage (SMES) in power systems with renewable energy sources," *IEEE International Symposium on Industrial Electronics*, p. 2487–2492.

[42] Z. Melhem, High Temperature Superconductors (HTS) for Energy Applications, Cambridge, U.K: Woodhead, 2012.

[43] M. Murname and A. Ghazel, "A Closer Look at State of Charge (SOC) and State of Health (SOH) Estimation Techniques for Batteries," Analog Devices, [Online]. Available: http://www.analog.com/media/en/technical-documentation/technical-articles/A-Closer-Look-at-State-Of-Charge-and-State-Health-Estimation-Techniques-....pdf. [Accessed 14 março 2018].

[44] MIT - Massachusets Institute of Technology, *A Guide to Understanding Battery Specifications*, MIT Electric Vehicle Team, 2008.

[45] B. B. McKeon, J. Furukawa and S. Fenstermacher, "Advanced lead-acid batteries and the development of grid-scale energy storage systems," *Proc. IEEE, vol. 102, no. 6,* p. 951–963, June 2014.

[46] M. T. Lawder, B. Suthar, P. W. C. Northrop, S. De, C. M. Hoff, O. Leitermann, M. . L. Crow, S. Santhanagopalan and V. R. Subramanian, "Battery Energy Storage System (BESS) and Battery Management System (BMS) for Grid-Scale Applications," *Proceedings of the IEEE , Vol. 102, No. 6,* pp. 1014-1030, June 2014.

[47] D. Kumar, S. K. Rajouria, S. B. Kuhar and D. K. Kanchan, "Progress and prospects of sodium-sulfur batteries: A review," *Solid State Ionics, Volume 312,* pp. 8-16, 1 December 2017.

[48] P. Vanýsek and V. Novák, "Redox flow batteries as the means for energy storage," *Journal of Energy Storage, Vol. 13,* pp. 435-441, October 2017.

[49] M. Conte, A. Iacobazzi, M. Ronchetti and R. Vellone, "Hydrogen economy for a sustainable development: state-of-the-art and technological perspectives," *Journal of Power Sources Volume 100, Issues 1–2,* pp. 171-187, 30 November 2001.

[50] G. L. Soloveichick, "Regenerative fuel cells for energy storage no. 6," *Proc. IEEE, vol. 102,* p. 964–975, June 2014.

[51] M. Aneke and M. Wang, "Energy storage technologies and real life applications—Astate of the art review," *Applied Energy, vol. 179,* p. 350–377, October 2016.

[52] "Thermal energy storage-technology brief.," *IEA-ETSAP and IRENA technology brief.*, 2013.

[53] European Commission - Directorate-General for Energy, "The future role and challenges of Energy Storage," *DG ENER Working Paper* , 2012.

[54] R. Morgan, S. Nelmes, E. Gibson and G. Brett, "An analysis of a large-scale liquid air energy storage system," *Proceedings of the Institution of Civil Engineers*, p. 10, 3 February 2015.

[55] U. D. o. Energy, Grid Energy Storage, 2013.

[56] M. Aneke and M. Wang, "Energy storage technologies and real life applications – A state of the art review," *Applied Energy, Volume 179*, pp. 350-377, 1 october 2016.

[57] A. T. C. d. F. Silva, "Design of the Storage capacity of artificial reservoirs," Universidade Técnica de Lisboa, Lisboa, 2010.

[58] V. Klemes, "Storage-Mass-Curve Analysis in a Systems-Analytic Perspective," *Water Resources Reseach, Vol. 15 - N°2*, p. 12, April 1979.

[59] T. A. McMahon and R. G. Mein, Reservoir Capacity and Yield, Clayton, Australia: Elsevier, 1978.

[60] S. M. Villela and A. Mattos, Hidrologia Aplicada, McGraw-Hill, 1979.

[61] V. Klemes, "Storage Mass-Curve Analysis in a Systems-Analytic Perspective," *Water Resources Research, Vol. 15 - N°2*, p. 12, April 1979.

[62] I. R. B. Santos, G. L. T. Filho, O. H. d. S. Júnior, B. T. C. Vasconcellos and F. J. d. Azevedo, "Análise Hidráulica para o ganho de capacidade de armazenamento em reservatório por meio do alteamento de um vertedouro lateral.," *XXIV SNPTEE - Seminário Nacional de Produção e Transmissão de Energia Elétrica.*, p. 8, 22-25 October 2017.

[63] R. d. L. Lucena, "Aplicações de um Método de Penalização Adaptativa em Sistemas Imunólogicos Artificiais para a Otimização de Problemas com Restrições," UFRJ, Rio de Janeiro, 2011.

[64] J. Brooks, "Distributed Coordination of Smart Loads to Provide Ancillary Service to the Power Grid," in *Dissertation, University of Florida*, Gainesville, 2017, p. 98.

[65] Y. Yang, S. Bremner, C. Menictas and M. Kay, "Battery energy storage system size determination in renewable energy systems: A review," *Renewable and Sustainable Energy Reviews*, vol. 91, pp. 109 - 125, 2018.

[66] IEEE Standards Association, *1013-1990 - IEEE Recommended Practice for Sizing Lead-Acid Batteries for Photovoltaic (PV) Systems*, 1990.

[67] A. Cervone, G. Garbone, E. Santini and S. Teodori, "Optimization of the battery size for PV systems under regulatory rules using a Markov-Chains approach.," *Renewable Energy*, vol. 85, pp. 657 - 665, 2016.

[68] J. Wu, B. Zhang, H. Li, . Z. Li, Y. Chen and X. Miao, "Statistical distribution for wind power forecast error and its application to determine optimal size of energy storage system," *Electrical Power and Energy Systems,* vol. 55, pp. 100 - 107, 2014.

[69] M. Yue and X. Wang, "Grid Inertial Response-Based Probabilistic Determination of Energy Storage System Capacity Under High Solar Penetration," *IEEE TRANSACTIONS ON SUSTAINABLE ENERGY,* vol. 6, no. 3, pp. 1039 - 1049, 2015.

[70] H. Bludszuweit and J. A. D. Navarro, "A Probabilistic Method for Energy Storage Sizing Based on Wind Power Forecast Uncertainty," *IEEE TRANSACTIONS ON POWER SYSTEMS,* vol. 26, no. 3, pp. 1651 - 1658, 2011.

[71] R. M. R. V. d. Ovelha, "Projeto, Dimensionamento e Instalação de Solução Fotovoltaica numa moradia offgrid," *Universidade de Lisboa, Dissertação de Mestrado,* p. 102, 2017.

[72] Y. Ru, J. Kleissl and S. Martinez, "Storage Size Determination for Grid-Connected Photovoltaic Systems," *IEEE TRANSACTIONS ON SUSTAINABLE ENERGY,* vol. 4, no. 1, pp. 68 - 81, 2013.

[73] P. Li, R. Dargaville, F. Liu, J. Xia and Y.-D. Song, "Data-Based Statistical Property Analyzing and Storage Sizing for Hybrid Renewable Energy Systems," *IEEE TRANSACTIONS ON INDUSTRIAL ELECTRONICS,* vol. 62, no. 11, pp. 6996 - 7008, 2015.

[74] Y. Yang, H. Li, A. Aichorn, J. Zheng and M. Greenleaf, "Sizing Strategy of Distributed Battery Storage System With High Penetration of Photovoltaic for Voltage Regulation and Peak Load Shaving," *IEEE TRANSACTIONS ON SMART GRID,* vol. 5, no. 2, pp. 982 - 992, 2014.

[75] D. W. Gao, Energy Storage for Sustainable Microgrid, Academic Press, 2015.

[76] S. Bahramirad and H. Daneshi, "Optimal sizing of smart grid storage management system in a microgrid.," *2012 IEEE PES Innovative Smart Grid Technologies (ISGT),* pp. 1-7, 2012.

[77] J. P. Fossati, A. Galarza, A. M. Villate and L. Fontán, "A method for optimal sizing energy storage systems for microgrids," *Renewable Energy,* vol. 77, pp. 539 - 549, 2014.

[78] S. Chakraborty, T. Senjyu, H. Toyama, A. Y. Saber and T. Funabashi, "Determination methodology for optimising the energy storage size for power system," *IET Generation, Transmission & Distribution,* vol. 3, no. 11, pp. 987 - 999, 2009.

[79] DOE/NSRDB, "National Solar Radiation Data Base. Department of Energy," 2016.

[80] J. I. L. Seguel, "Projeto de um sistema fotovoltaico autônomo de suprimento de energia usando técnica MPPT e controle digital.," *Dissertação de mestrado, UFMG,* p. 222, 2009.

[81] SUNPOWER, "Datasheet SunPower E18/305 Solar Panel," 2010. [Online]. Available: https://us.sunpower.com/home-solar/solar-cell-technology-solutions/. [Accessed January 2018].

[82] Lazard, "Lazard's Levelized Cost of Storage Analysis - Version 4.0," 2018.

[83] L. U. Ribeiro Júnior, "Contribuições metodológicas visando a outorga de recursos hídricos para geração hidrelétrica.," *Dissertação de Mestrado,* p. 157, 2004.